Microscopic and macroscopic manifestations of percolation transitions in a semiconductor composite

D. Azulay,[1] O. Millo,[1] E. Savir,[1] J. P. Conde,[2,3,4] and I. Balberg[1]
[1]*The Racah Institute of Physics, The Hebrew University, Jerusalem 91904, Israel*
[2]*INESC Microsystemas e Nanotechnologias, Lisbon 1000-029, Portugal*
[3]*IN–Institute of Nanoscience and Nanotechnology, Lisbon 1000-029, Portugal*
[4]*Department of Chemical and Biological Engineering, Instituto Superior Técnico, Lisbon 1049-001, Portugal*
(Received 27 July 2009; revised manuscript received 5 October 2009; published 10 December 2009)

Using microscopic and macroscopic studies we have derived a comprehensive picture of the relation between the conduction routes and the transport mechanisms in the μc-S:H/a-Si:H composite system. In particular, we have established that in this system the increase of the fractional crystallite phase content, x, brings about two percolation transitions. In the first, at $x \sim 0.3$, the transport changes from being via the a-Si:H matrix to taking place via a three-dimensional conducting network consisting of Si microcrystallites that are embedded in the a-Si:H matrix. In the second, at $x \sim 0.7$, the dominant transport becomes associated with a two-dimensional network of the disordered silicon tissues that encapsulate the crystallite columns, which form with the increase of x. These two transitions define then three different x regimes which are, from the electrical connectivity point of view, very different from each other. In contrast, the carriers' transport and the carriers' recombination mechanisms are qualitatively quite similar, though quantitatively quite different, in each of the above regimes. Within the framework of this unified picture we are able now to explain various (in some cases contradicting) results that were reported in the literature in which only some aspects, applicable to limited x regimes, have been reported. In turn, the present work brings to light the richness of mechanisms and phenomena that are to be expected in semiconductor composites in comparison with their metal-insulator counterparts.

DOI: 10.1103/PhysRevB.80.245312 PACS number(s): 73.50.Gr, 64.60.ah, 72.80.Tm, 68.37.Ps

I. INTRODUCTION

The electrical properties of more-than-one phase systems have been discussed in the last few decades by percolation,[1] continuum percolation,[2] and effective medium (EM) theories[3] for systems where the natures of the involved phases were described by their single-phase macroscopic properties, such as their corresponding electrical conductivities. In particular, metal-insulator composites such as granular metals were intensively studied and are quite well understood.[4,5] However, even in these relatively simple systems a rich collection of phenomena is found due to the details of the local transport between two metallic grains and the various environments in which the grains are embedded. This richness is expected to be extended considerably in composites made of semiconductor phases since a greater variety of the geometrical and electronic structures, as well as transport mechanisms, can determine then the local and global transport properties of these systems. In particular, the combination of these mechanisms with the many alternative percolation networks yields very many resultant-macroscopic behaviors. For example, even in the simplest composite of two semiconductor phases, the interfaces between the particles of the same or different phase do not only affect the corresponding charge transfers between the particles but they themselves can constitute conducting networks in addition to the single-phase (percolation) or the two-phase (EM) conducting networks that exist in the systems. Moreover, the transport mechanism in each of those networks may be different, yielding, for example, a different temperature-dependent dominant conducting route in the system. While various aspects of semiconductor composites have been studied for a long time we do not know of a comprehensive-systematic picture of current routes and transport mechanisms in any of them. This is in spite of the fact that some classes of semiconductor composites became of great interest in recent years. This includes, for example, carbon nanotube composites,[6] porous semiconductors,[7] and semiconductor nanocrystallite ensembles in various insulating matrices.[8] The complexity that is associated with the expected richness of the phenomena makes, however, the understanding of such systems quite difficult. This is in particular so when only the macroscopic attributes are known; since then, it is not clear which of the possible available electrical networks in the system is the one that dominates the resultant-macroscopic behavior. Consequently, the amenability of the so concluded transport mechanisms is questionable. The lack of corresponding studies that attempt to correlate the transport routes with the electrical transport mechanism can be understood by the obvious complication that is involved in performing, simultaneously, macroscopic (to determine the transport mechanism) and local-microscopic (to determine the dominant current route) measurements. Noting that only such a combination may yield a full and self-consistent picture of the electrical properties of semiconductor composites, we try to demonstrate here the power of such a combined study by considering a nontrivial composite system in which more than a single semiconductor phase is included and in which more than a single conduction route is *a priori* possible.

Following the above considerations we have carried out a comprehensive-systematic study of the system of hydrogen-

ated microcrystalline-silicon (μc-S:H), where silicon microscrystallites are embedded in an hydrogenated amorphous silicon (a-Si:H) matrix.[9–11] This system is chosen because there were numerous studies of it and thus the conclusions to be derived here can have a relatively wide basis. Moreover, of course, this system is known to be of great basic physics and application interest. We will accompany then the presentation of our results with comparisons with corresponding data from the literature, having in mind the setting of a framework for future discussion of percolation phenomena in semiconductor composites.

As is well known the properties of the above system strongly depend on the relative content of the crystalline and amorphous phases. Correspondingly, while in the literature all the above composite systems are usually referred to as μc-S:H, it will be more accurate to refer to it (as will be done here) as the μc-S:H/a-Si:H composite. In this system the resultant-macroscopic dark conductivity, σ_d, was found, in quite a few works, to increase in "jumps" with the increase of the *partial volume content of the microcrystalline phase*, x. These jumps were either smeared[12–15] or abrupt,[16–22] and in almost all of the reported studies only a single "jump" was observed in a given study of the $\sigma_d(x)$ dependence. When characterized by the corresponding x values, the single jumps were identified to take place at $x \approx 0.3$ (Refs. 16 and 23) or at $x \approx 0.7$.[17–20] The reason that the reported $\sigma_d(x)$ dependence was almost always too blurred to even resolve if more than one percolation transition takes place with increasing x seems to be associated with the fact that in the preparation of the μc-Si:H/a-Si:H films the value of x is found to change considerably over a relatively narrow range of the deposition parameters.[12,19–22] Hence, usually, the dependence of σ_d on the crystallite content was not given in the literature in terms of x (Refs. 12, 14, and 16) but rather in terms of one or more of the controllable film deposition parameters which determine this value.[19–26] In particular, the degree of the dilution of the silane (SiH_4) gas by molecular hydrogen (H_2) during the deposition of the composite films is the most commonly used parameter to characterize the variation of x.[19,21,24,25]

Following the recognition of the existence of the above two transitions[20] their nature was discussed only in the general phenomenological terms of EM[27] or percolation[16] theories, but with no accompanying evidence as to the nature of the corresponding percolation networks.[16] In particular, in almost all of the corresponding studies[16,28] no correlation was attempted between the suggested transport mechanism and the particular phase or current network for which these models have been proposed. The common model that was applied was either that of a mixture of crystallites in an a-Si:H matrix, assuming that structurally the system is basically similar to that of granular metals,[17,29] or that of a system that is very similar to polycrystalline silicon (PSi).[12,15,30–33] In fact, the discussions were usually limited to a particular percolative phase that was assumed to be involved, while no reference as to the role of the corresponding value of x was made. We note in passing that corresponding behaviors were also manifested by the optical properties[34,35] of the systems. However, and most importantly, while many data were gathered, no complete account of the evolvement of the transport and recombination mechanisms of the electronic system with x has been given yet. In particular, while structural information and macroscopic transport measurements of this system were reported, no combined determination of the current routes and the macroscopic transport properties has been reported and thus the attribution of a given transport mechanism to a particular component of the network has not been established. This problem is very significant in systems such as μc-Si:H/a-Si:H since the main tool for the determination of the transport mechanism is the temperature dependence of the dark conductivity, $\sigma_d(T)$. As such, this tool does not yield unique conclusions[36] and the controversy regarding the transport mechanism in the μc-Si:H/a-Si:H composite still exists[11] and, essentially, every possible mechanism has been already proposed for this (usually, with no specific value of x) system. As we will try to argue upon the presentation of our results, *only a combination of the* $\sigma_d(T)$ data with additional information can significantly narrow down the number of possible transport scenarios. We believe that, in turn, our present and previous[37–39] detailed characterizations of the low-x and high-x phases enable now to set a self-consistent framework for the discussion of the μc-Si:H/a-Si:H system and for the interpretation of the many results reported in the literature and in particular the $\sigma_d(x)$ dependence. Also combining the data presented here and a critical examination of the previous literature has enabled us then to draw new conclusions regarding the transport mechanism in the μc-Si:H/a-Si:H system as follows.

(1) For all values of x the system is essentially a disordered semiconductor in which the conduction is determined by transport in band tails. The different temperature dependencies of the conductivity, in the three x regimes, are only due to differences in the density of states (DOS) distribution in the mobility gap in them. We suggest then that in spite of the very different topologies and current routes of the various x regimes the very basic electrical transport mechanism in all of them is the same.

(2) We clearly show that the recombination process varies also between the three x regimes and that its behavior is intimately associated with the transport behavior.

(3) The less studied and less discussed intermediate-x regime is shown to be a prototype of a semiconductor composite in which the transport is determined by a percolation network on the one hand and semiconductor interfaces on the other hand.

(4) The percolation transitions and their character, which have been hardly discussed before, are shown to be the defining borders of the various state distributions and consequently of the corresponding transport and recombination mechanisms.

(5) The role of oxygen as a dopant and a defect in the μc-Si:H/a-Si:H system is revealed microscopically.

In the present work the microscopic studies were conducted with the local probe measurements of conductive atomic force microscopy (C-AFM) as well as with scanning tunneling microscopy (STM) in the scanning tunneling spectroscopy (STS) mode. For the macroscopic study we have studied the $\sigma_d(x,T)$ as well as the photoconductivity, $\sigma_{ph}(x,T)$, dependencies for undoped and doped samples (in order to be able to map the entire-x range and to clearly

identify the two transitions). The latter dependencies were also used to show how both the transport and the recombination mechanisms change as the system goes through the two percolation transitions. In particular, the combination of the two dependencies has enabled us to distinguish between the mobility-connectivity and the carrier concentration aspects of the macroscopic electrical conductivity.

We have pointed out above that, essentially, quite a few possible mechanisms have been proposed for this system and that the modus operandi of previous works was usually to present *ad hoc* models for their specific experimental results (for a specific or unknown x). This was without providing a critical examination of the consequences of the suggested model and without making comparisons with results and/or models of others. In the present work we tried to critically examine our results in light of the various possible models in order to narrow down the number of applicable scenarios and thus to overcome the still existing widely discussed controversy regarding the transport mechanism.[11]

The structure of this paper is as follows. In Sec. II we describe briefly the sample preparation and the experimental techniques used for the macroscopic and microscopic measurements noting that these were detailed in our previous works on the $x \approx 1$ phase.[37,38] The experimental results that are given in Sec. III are presented in an order that enables to follow both the fundamental and the side issues of the evolvement of the charge transporting network with the increase of x in the presently studied μc-Si:H/a-Si:H systems. We accompany this presentation with discussions on the meaning of the particular experimental findings with the aim to narrow down the number of scenarios that were suggested by the many previous works. This, in turn, will also enable us to set the framework that we try to establish in Sec. IV. In Sec. IV we will present then the emerging picture of the transport networks and summarize the corresponding transport and recombination mechanisms in the three types of networks that emerge as x is increased. The self-consistent model that seems to be provided by the present study is expected to guide future transport studies of semiconductor composites, in general, and set the arena for a systematic interpretation of results reported in the literature on the so widely studied μc-Si:H/a-Si:H system in particular.

II. EXPERIMENTAL

The μc-Si:H/a-Si:H films used in the present study were deposited, as described in detail previously,[24,40] by the hot-wire chemical vapor deposition (HW-CVD) technique. The thickness of the films, which were deposited on a Corning 7059 glass, was about 0.5 μm. The common substrate temperature during the deposition of all the films used in the present study was 175 °C and the pressure of the flowing gas mixture, of molecular hydrogen (H_2) and silane (SiH_4), was 20 mTorr. No significant differences were found between these films and the films that we used in our previous studies[37–40] and which were 1 μm thick. We have determined the oxygen content in the samples by both secondary ion mass spectroscopy and the relative infrared absorption of the Si-O band at 1150 cm^{-1}. The oxygen content estimated in all our films was of the order of 10^{18} cm^{-3}, typical for μc-Si:H samples prepared by the HW-CVD techniques.[41] Following the well-known fact that the degree of H_2 dilution of the SiH_4 gas, during the deposition process, determines the concentration of the crystallites in the films,[18,19,21,22] we have varied the degree of the dilution $y = 100[H_2]/[H_2 + SiH_4]\%$ from $y = 0\%$ (yielding a "pure" a-Si:H-like phase[39]) to $y = 95\%$ (yielding, what we call, a pure microcrystalline, μc-Si:H, phase[38,39]). The doping of the samples, when desired, was achieved by the mixing of the silene with 1 vol % of phosphine (PH_3).

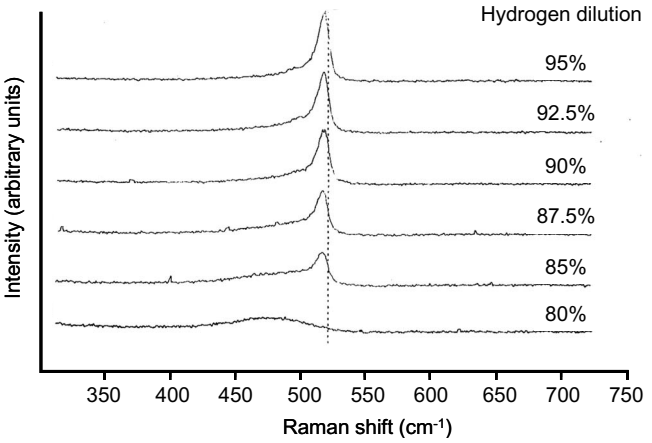

FIG. 1. The Raman spectra of our μc-Si:H/a-Si:H samples for films that were deposited under different H_2 dilutions, y, as indicated in the figure. Note that up to $y = 80\%$ there is no trace of Si crystallites and above 87.5% there is hardly any trace of a-Si:H.

As pointed out in Sec. I the relative content of the crystalline phase x is well established to vary monotonically with the variation of the H_2 dilution parameter y.[19,21,24,25] It was realized at an early stage of the studies of the μc-Si:H/a-Si:H system that the Raman scattering can serve as a common procedure to evaluate the value of x.[9] In this method the ratio between the "strength" of the crystalline silicon transverse optical (TO) band at 521 cm^{-1}, I_c, and the strength of the corresponding amorphous band at 480 cm^{-1}, I_a, is considered to account for x.[40,42] In fact the ratio $I_c/(I_c + I_a)$ became synonymous with x in the later literature.[16,20] The fact that the value of $x \approx 0.7$ is very reasonable for the corresponding transition (see Sec. IV) and the fact that the relation that this method provides between the x and the known y values are found to be the same by different groups,[15,18,19,22,24,25] give us confidence that Raman spectroscopy yields a reliable "universal" scale for the presentation of the data obtained as a function of x. Following the above it is apparent that for the consideration of our results within the framework of percolation, on the one hand, and in order to establish a common ground with results obtained by others, on the other hand, the determination of the x values is essential and thus we turned to the application of the Raman scattering to a series of samples that were produced under conditions that are identical to the ones in the present study. The results of our micro-Raman scattering measurements for some y values used in the present study are shown in Fig. 1. As seen, at $y = 80\%$ (of H_2 dilution) there is no detectable trace of the crystalline TO band, yielding exactly the same

spectrum that we obtained previously[44] for the pure (i.e., $y=0\%$) *a*-Si:H phase. The detection of the TO band for $y=85\%$ clearly indicates that crystallites are formed as y increases between 80% and 85%. We can further conjecture that crystallite forms in the 0–80 % interval, and thus, while we cannot attribute a specific x to results obtained in this interval we could expect, in view of the above discussion, that x increases monotonically with y in it. Similarly, for $y \geq 92.5\%$, the amorphous silicon (480 cm^{-1}) band is hardly detectable indicating that only minute amounts of the *a*-Si:H phase exist in the corresponding samples. We can however conjecture, as above, without knowing the exact value of x that it increases with y in the latter range. Only the samples that were deposited under intermediate dilutions, $80\% < y \leq 90\%$, contain both phases and their x values were estimated by our Raman spectroscopy analysis[24,40] to be in the $0.3 \leq x \leq 0.7$ regime. These x value estimates, as pointed out above, are in agreement with our own structural data (see below) as well as with the many similar estimates that have been derived by other authors.[15,22] In particular, such dependence (for one of the transitions) with more experimental points (using the variation of another deposition parameter) was reported by another group.[16] In view, however, of the above mentioned hardship (in particular the narrow y range) to prepare samples with many distinct intermediate-x values between 0.3 and 0.7, we could, as in previous studies,[14–16,22,27] determine the percolation thresholds but we could not follow the functional critical behavior of the conductivity just above the transitions, as we were able to do for other systems.[2,45] For the above y range we found that the $y=82.5\%$, 85%, 87.5%, and 90% values correspond to the 0.3, 0.4 0.5 and 0.7 x values, respectively. Considering the effect of the other deposition parameters we can, following our many previous studies,[24,40] assume that the above values appear to be amenable within $x \pm 0.1$ and that the low-x transition takes place always in the $y=80-82.5$ % interval.

In trying to discuss the transport data in the μc-Si:H/*a*-Si:H system as a function of x we encounter then two difficulties. For the $x<0.3$ and the $x>0.7$ regimes we do not know the $x(y)$ relation, while for the $0.3<x<0.7$ regime (following the hardship to prepare many distinct intermediate-x samples within the corresponding narrow y range) we have only very few $x(y)$ values. However, as in previous studies the rather few x values in the latter regime were enough to determine, with a reasonable accuracy of the x values, the percolation thresholds.[14–16,22,28] On the other hand, trying to set a framework for the entire μc-Si:H/*a*-Si:H system (i.e., not only in the $0.3<x<0.7$ interval) we could identify the samples on which the corresponding data were taken only by their y values. Correspondingly, we will present the various data here as a function of y and, when appropriate, interpret them in terms of x. Many more details on the sample preparation, the estimate of the crystallites size from the Raman spectra, and some electrical and optical properties of the films, such as those used in the present study, can be found in Refs. 20, 40, and 42.

Our macroscopic conductivity and photoconductivity measurements were carried out in the photocarrier grating (coplanar) configuration that we have described in detail previously.[37,39] A two-probe configuration (evaporated silver strips separated by 0.4 mm) was used for these rather standard measurements in the dark and under illumination. The current-voltage characteristics (for all the samples used here) were linear in the 0–100 V range that was used throughout the present study. In order to get further information on the transport and the recombination mechanisms all the conductivity and photoconductivity measurements were carried out at temperatures ranging between 78 and 300 K as described previously.[37,39] It should be pointed out that the dark resistivity of the undoped samples was too high to monitor at lower temperatures. Hence, as in many previous studies[15,17,18,27–29,33] we have usually derived the corresponding activation energy of the dark conductivity (E_a, see below) only in the upper part of this range. To overcome this problem, at least partially, we have conducted the same study on phosphorous mildly doped samples. We expected, following previous works[46] and as will be confirmed in this study, that this level of doping (see above) will not change in any significant way the structure of the system.

For the measurement of the photoconductivity, a He-Ne laser illumination was applied enabling a maximum carrier generation rate, G, of 10^{21} cm^{-3} s^{-1}. For the determination of the dependence of the photoconductivity on the illumination intensity, we have varied G between the above value and 10^{19} cm^{-3} s^{-1}. These conditions are, again, the same as the ones we have used in our detailed phototransport studies of *a*-Si:H (Ref. 39) and the pure μc-Si:H (Ref. 37) phases. Following the fact that in the present study we limit ourselves to demonstrate that the recombination mechanisms vary through the two percolation transitions, without going into the particular lengthy details of the mechanism (that requires a separate very elaborate study, as we did in our previous works[37,39]), we will present here only the y (or x) dependence of the photoconductivity σ_{ph} and the light intensity exponent γ_e. The latter quantity is derived from the relation $\gamma_e = d[\ln(\sigma_{ph})]/d[\ln(G)]$, following the well-known common power-law dependence of σ_{ph} on G.[47] Correspondingly, the γ_e values that we report here (in contrast with our previous works[37,39]) are only those of the majority carriers (here the electrons). We note in passing that the γ_e values are very informative since they are related only to the recombination mechanism[47] as reflected by the recombination time τ_e ($=\sigma_{ph}/Ge\mu$, where μ is the electron mobility and e is the electronic charge). Hence, the variation of γ_e with x will indicate in the present study the corresponding variation of the recombination mechanism. Our approach will be then to combine the derived parameters σ_d, σ_{ph}, E_a, and γ_e with the information on the current route maps, which we determine by the local probe measurements, for the evaluation of both the transport and the recombination mechanisms in the possible networks of the μc-Si:H/*a*-Si:H composites.

In our microscopic measurements, we examined the local structural and local electrical properties by employing C-AFM in the contact mode with a conductive metal-coated Si tip having a force constant of typically 0.03 N/m and a radius of curvature that is less than 35 nm. The application of a corresponding attachment to our AFM system (NT-MDT Solver) has enabled us to obtain high resolution images of the currents through the system and a reconfirmation of the interpretation we suggested following our previous C-AFM

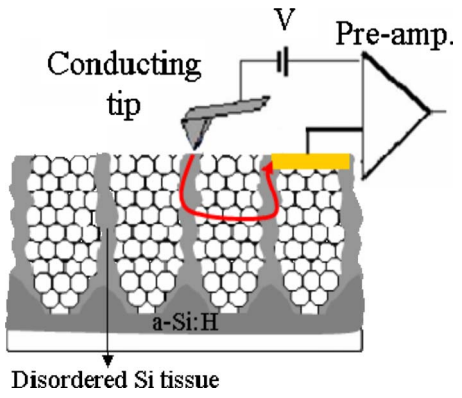

FIG. 2. (Color online) An illustration of the C-AFM configuration used in the present study when applied to the structure of the nearly pure μc-Si:H phase ($x \rightarrow 1$). In this illustration the current routes between the tip and the evaporated electrode (that connects to the preamplifier) are assumed to be dominated by the percolation network that consists of the "envelops" (the light gray areas) of the crystallites columns.

and STM measurements.[38] We have carried our C-AFM measurements in both a "vertical" configuration (where the counterelectrode to the C-AFM tip was an underlying Au/Cr film that was predeposited on the substrate) and a "lateral" configuration (in which the counterelectrode was a gold strip evaporated onto one edge of the μc-Si:H/a-Si:H film). In the latter configuration, which is illustrated in Fig. 2 for the columnar structure that exists for the high-x range of the μc-Si:H/a-Si:H system,[9,20,38,48] the tip scanned a region that is a few mm away from the above gold strip. Hence, the detection of the current indicated the existence of a macroscopic-percolative current route between the tip and the strip. In Fig. 3 we see that the high resolution AFM reveals the structure of columns and the presence of the encapsulated crystallites within them. The former are shown to have a width of about 130 nm and the latter are about 20 nm in diameter. This is in agreement with previous findings of us[38] and others[15,18,49,50] on similar systems.

Unlike our previous study,[38] where we used the STM only for the derivation of structural characteristics and current images, in the present study we have mainly used the STM apparatus to perform tunneling spectroscopy.[51] In this mode we were able to measure the current-voltage characteristics that hold information regarding the DOS distribution in the

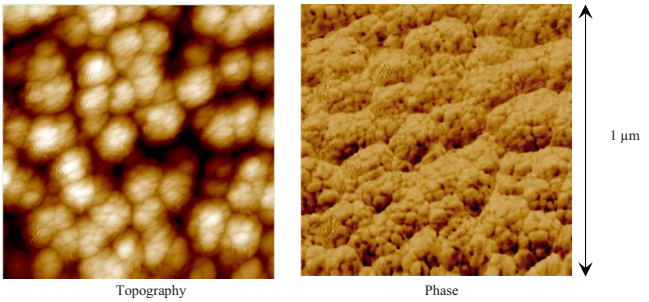

FIG. 3. (Color online) AFM topographic (left) and phase (right) images as obtained on the $x \approx 1$ phase. The height range in the topographic image is 35 nm.

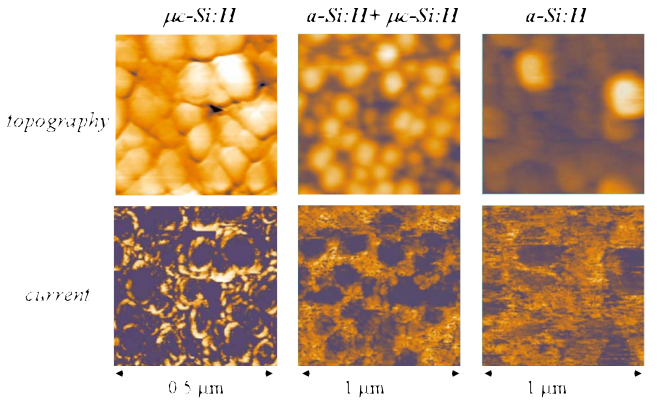

FIG. 4. (Color online) Typical topography and current images of the a-Si:H/μc-Si:H systems in the pure μc-Si:H phase (left), the intermediate ($x \approx 0.5$) phase (middle), and the pure a-Si:H phase (right). The currents in the latter phase are more than one order of magnitude smaller than those via the CETs. Topography range, 30 nm; current ranges, 15 nA at $V=-3$ V (left), 0.35 nA at 9 V (middle), and 0.2 nA at 10 V (right).

mobility gap of a semiconductor. This was possible, however, only for our most conducting samples, i.e., for the pure (or almost single-phase) μc-Si:H samples.

III. EXPERIMENTAL RESULTS AND THEIR ANALYSIS

A. AFM and C-AFM studies

Following our emphasis on the need to be familiar with the carrier transporting networks, already at the start, we review first the current routes that we have determined in the structures that we obtained for the μc-Si:H/a-Si:H systems. Defining the basic three x regimes of the composites by the above mentioned two conductivity transitions we show in Fig. 4 the C-AFM images of the $x \approx 1$ (μc-Si:H), $x \approx 0.5$, and $x \approx 0$ (a-Si:H) contents. While we could resolve the current via the single crystallites in the first regime (by using a tunneling high sensitivity C-AFM module; see Fig. 5 below) we were unable to do so in the latter two regimes. Noting

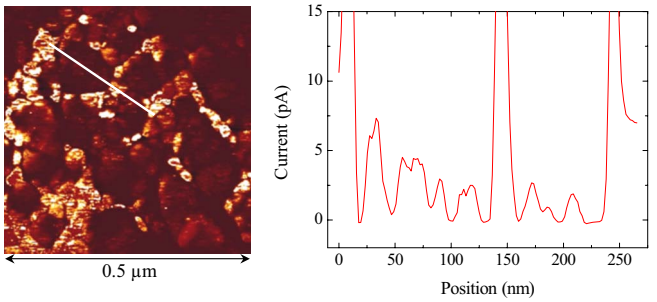

FIG. 5. (Color online) Current image of a pure μc-Si:H phase ($x \approx 1$) measured with a high sensitivity C-AFM module, and a current cross section along the line shown in the figure. Note that the dominant transport is via the columns encapsulating tissue but smaller currents through the encapsulated individual crystallites are also detected. The voltage applied was 5 V and the current range was 0–100 pA (module saturation current).

that the images of Fig. 4 were taken in the lateral configuration, the observation of the currents in the pure μc-Si:H phase indicates that the columns are well connected electrically to the counterelectrode, via a percolation network, as was illustrated in Fig. 2. We can look then at the crystallites as being encapsulated within columns, and following previous works of us[37,38] and others[48,52,53] we can assume that this encapsulation is by a disordered Si tissue (see also below). Correspondingly, we will call these "edges" of the crystallites' columns the columns encapsulating tissues (CETs). As in our previous study[38] we see in Fig. 4 here that in the $x \approx 0$ (i.e., the a-Si:H-like phase) such columns are not present at all, while in the $x \approx 0.5$, intermediate-x μc-Si:H/a-Si:H regime, the columns that have already been formed are not yet geometrically or even electrically connected.[38] In the latter x regimes we expect then that the lateral microscopic conductance that we measure is not associated with the columns. On the other hand, following the fact that the macroscopic conductivity in the intermediate-x regime is larger than that of the a-Si:H matrix,[12,16,54] as will be shown below for our samples, we argue that in this (rather unexplored) intermediate-x regime[17,34,55] the major contribution to the global transport is due to *conduction in which Si crystallites* are involved.

Returning to the high-x regime, we note that the picture proposed by us[38] and also confirmed later by another group[49] is in contrast with the conclusions of a work[50] that preceded ours, i.e., that the dominant current takes place via the crystallites within the columns. Following this apparent contradiction we carried out in the present study a high sensitivity C-AFM study that enabled us to separate more clearly these two contributions. Indeed, the corresponding result that is shown in Fig. 5 reveals that the C-AFM detects not only the relatively larger currents in the CETs but also the much smaller currents within the columns that are clearly associated with the microcrystallites. In passing, we note that the corresponding images show again (and now electrically) that the size of the crystallites is about 15–25 nm, and this, as mentioned above, is in excellent agreement with our Raman, AFM (Fig. 3), and STM data.[38] The important observation is however that the current image and the line section in it clearly demonstrate that in the $x \rightarrow 1$ regime *the dominant currents passing via the columns encapsulating tissue are one order of magnitude larger than the currents through the individual crystallites.* Possible reasons for the difference between the results in Ref. 50 and our results will be discussed in Secs. III D and IV. However, already at present we can safely conclude that the conductivity rise that we and others[15,17,22] found at $x \approx 0.7$ is associated with *the onset of transport in a lateral continuous network of the CETs*. From a percolation point of view this network is then a two-dimensional-like system of "circles".[2,38]

It is important to note that, in principle, one may argue that the observed higher current that we found at the edges of the columns, in the C-AFM measurements, is an experimentally induced rather than an intrinsic effect. For example, the AFM tip may make a better contact at the edge of the columns or that at the top of the columns the tip can cause a more efficient anodization of the inner crystallites than of the outer crystallites, such that the surface oxide that forms is thinner at the "edge" crystallites. We took quite a few precautions to confirm that these scenarios do not apply in our work. This was done by carrying out the measurements before and after a diluted-HF etching of the samples, by performing the scans in two opposite directions and under two bias polarities as well as by carrying out the measurement also in a ultrahigh vacuum system (variable temperature UHV-STM/AFM Omicron). Finding no significant changes in the images we concluded that indeed neither of the above possible scenarios applies in our study. As an example for that one can see that the image shown in Fig. 4 for the $x \rightarrow 1$ regime, taken here at a negative bias, is similar to the image that we have shown previously[38] for that system for a positive bias. However, the most convincing evidence that shows that we do not have here any tip-surface contact effect follows from our previous current imaging tunneling spectroscopy[51] measurements[38] that have clearly shown higher currents at the column boundaries. This is since the latter is a *contactless current* spectroscopy technique and thus tip-surface effects are clearly avoided.

We can then finally conclude that the low x (≈ 0.3) conductivity transition is associated with the evolution of a silicon crystallite network (as found from the Raman data) and that the conductivity transition at the high-x (≈ 0.7) value is associated with the formation of a continuous network of joint CETs. Following that, we can identify now the structure variations that are associated with the two conductivity transitions that we mentioned in Sec. I. The first transition, as will be further discussed below, is reminiscent of the percolation transition in granular metals,[4,45] while the other conductivity transition, at $x_{c2} \approx 0.7$, is from that of the "mixed phase" (that may contain some "disconnected" columns) to the network of connected columns, where the CET network dominates the conduction. Following those structural-electrical information we turn now to show that the above conclusions from the microscopic study are also confirmed by the variations in the macroscopic transport and recombination properties.

B. Temperature dependencies of the transport and phototransport properties

Establishing the existence of the three principal x regimes from the geometrical and electrical connectivity points of view, we will try now to evaluate the very basic transport and recombination mechanisms in each of these regimes. Our main aim is to establish that the observed conductivity transitions separate three electrically distinguishable phases that are defined by the presence of *two genuine percolation transitions* (at $x \approx 0.3$ and at $x \approx 0.7$; see above). This will be done here by examining the transport properties, as derived from $\sigma_d(T)$, and the recombination properties, as reflected in the $\sigma_{ph}(T)$ dependencies. Noting, however, that these macroscopic behaviors are not enough to lead to a unique determination of the corresponding mechanisms, we will reduce the number of possible such scenarios by a comparison of the results that we obtained in the three regimes. The particular additional properties that we will examine are the x depen-

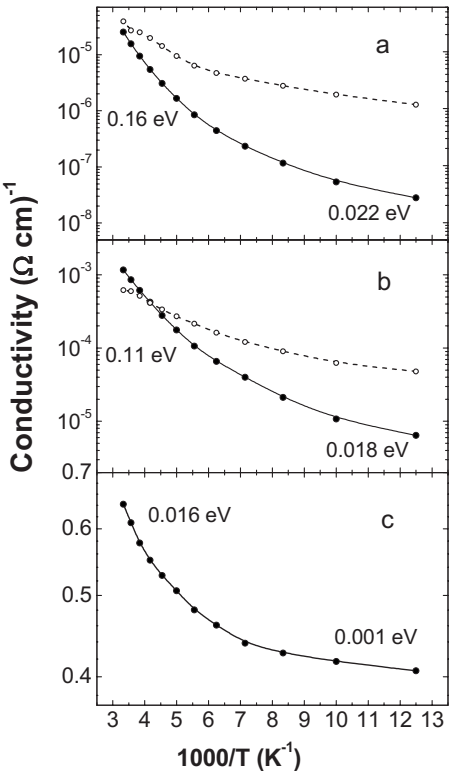

FIG. 6. An Arrhenius presentation of the temperature dependence of the dark conductivity (full dots) and photoconductivity (empty dots) in the P-doped samples of (a) $y=50\%$, (b) $y=90\%$, and (c) $y=95\%$. The E_a values corresponding to the lowest and highest temperatures are denoted in each panel.

dencies of dark conductivity activation energy, E_a, and the light intensity exponent, γ_e. For the comprehensiveness of the present study and for the possibility to carry out a comparison between our results and results in the literature, we report here measurements on both undoped and doped samples, noting that from the structural point of view, the very mild doping used here ($PH_3/Si:H_4=10^{-2}$) ensures that the systems are structurally the same.[46]

In order to exhibit the $\sigma_d(T)$ and the $\sigma_{ph}(T)$ data for all the three x regimes identified above (considering the above mentioned high resistance limitations of the low-x regime) we start by showing the results of our macroscopic study as obtained on the doped samples. These results are presented in Fig. 6 by Arrhenius plots because this is the most common way to present such data and since, as will be discussed later, it is the most appropriate presentation for our interpretation. This presentation assumes that $\sigma_d(T)=\sigma_0 \exp[-(E_a/kT)]$, where σ_0 is a system parameter, E_a is the activation energy, and kT is the thermal energy. The most significant feature of $\sigma_d(T)$ is the increase of the value of E_a with temperature. These values at the extreme ranges of the considered temperatures are indicated in the figure. We note of course that while the E_a (300 K) values are expected to be meaningful, the diminishing E_a (80 K) values appear to merely indicate the transition to a nonactivated conductivity behavior (see below). We also note that if the E_a values would have been derived from the $\sigma_{ph}(T)$ dependence they would be systematically smaller than those derived from the $\sigma_d(T)$ dependencies. In Fig. 6(a) we show then the $\sigma_d(T)$ and $\sigma_{ph}(T)$ dependencies for the $y=50\%$ ($x<0.3$) sample which is "essentially" a system in which the transport is dominated by the a-Si:H phase. In this figure the photoconductivity $\sigma_{ph}(T)$ shows a very mild temperature dependence, which is reminiscent of the results obtained in crystalline and amorphous semiconductors[47,56–58] albeit without the conspicuous photoconductivity peak which is a signature of the contributions of the dangling bonds in a-Si:H.[39,56,59] We note, however, that this is not unexpected since the H_2 dilution appears to quench this "dangling bond peak" in a-Si:H, indicating that the DOS is dominanted by the band tails.[60]

Turning to the intermediate-x phase of $y=87.5\%$ ($x\approx0.5$), we see in Fig. 6(b) a behavior that is similar to that of Fig. 6(a), but the values of $\sigma_d(T)$ and $\sigma_{ph}(T)$ are systematically larger and the values of E_a are systematically smaller than in the above a-Si:H-like case. On the other hand, as shown in Fig. 6(c), while the same trend is maintained on turning to the columnar structure, at $y=95\%$ ($x\approx1$), a dramatic increase in σ_d takes place. This is a clear indication that the CET is an entity that is readily dopable, not only by oxygen but also by other donors, yielding a heavily doped bulklike semiconductor. This can be well understood by the effect of gettering of the intercrystallite boundaries as found in polycrystalline silicon,[61] such that, when doped, the encapsulating disordered tissue in this high-x system may even be referred to as a "dirty metal."[62]

In the undoped samples we could measure the $\sigma_d(T)$ dependence only for the intermediate and high-x regimes and then only over the upper part of our temperature range. The facts that for the $x<0.3$ regime we could not measure this conductivity and that the $\sigma_{ph}(T)$ dependence found is similar to that of the pure a-Si:H phase[11,39,59,63] justify our above suggestion that in the corresponding low-x regime the a-Si:H phase dominates the transport and phototransport. The results of the $\sigma_d(T)$ (measured only above 180 K) and $\sigma_{ph}(T)$ measurements for the $x>0.3$ phases are shown then in Fig. 7. The E_a values (extracted, though, from a very narrow temperature range) for both $y=87.5\%$ [Fig. 7(a)] and $y=95\%$ [Fig. 7(b)] samples are much higher compared to the values in the corresponding doped samples (Fig. 6). The photoconductivity of the $y=87.5\%$ sample here is reminiscent of our findings in Fig. 6(b) and with works of others[54] that were probably concerned with this regime. In Fig. 7(b) we saw that qualitatively similar results were obtained for $y=95\%$. These results are indeed similar to results obtained by others for this regime before.[64] For the discussion below we should note that the results in Fig. 7 follow the same trend that we found in Fig. 6.

In order to provide a unified framework for the discussion of the corresponding transport mechanisms, on the one hand, and to justify the Arrhenius data presentation in Figs. 6 and 7, on the other hand, let us compare our data with those given in the literature for the μc-Si:H/a-Si:H system. However, noting that there are numerous published $\sigma_d(T)$ data, we will only mention here representative examples. The four conspicuous mechanisms that one encounters in the literature for the interpretation of the $\sigma_d(T)$-like data in previous works on μc-Si:H/a-Si:H composites are (i) thermionic emission over barriers between adjacent semiconductor

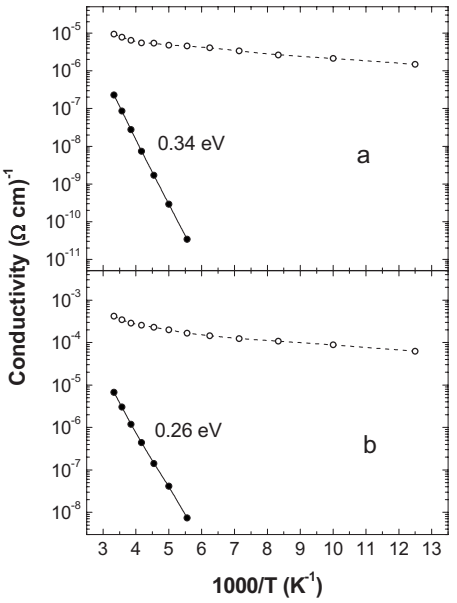

FIG. 7. An Arrhenius presentation of the temperature dependence of the dark conductivity (full dots) and photoconductivity (empty dots) in the undoped samples of (a) $y=87.5\%$ and (b) $y=95\%$. The corresponding activation energies are denoted in each panel.

crystallites,[17,27,32,65–67] (ii) thermally activated tunneling,[68] (iii) variable range[28,62,69] or near neighbor[70] hopping, and (iv) temperature induced variation of the Fermi level position, E_F, throughout the landscape of the state distribution in the mobility gap. This is, as in *a*-Si:H,[71] usually through band tails.[11,18,20,72,73] We note in particular that various versions of the latter were suggested for x values that we correlate here with the low x,[18] the intermediate x,[43,74] and the high-x (Refs. 18, 52, and 75–78) regimes. Some works have even suggested a combination of two of the above scenarios.[33,63,79,80] We must point out though that of the numerous works that reported the $\sigma_d(T)$ dependence, in various μc-Si:H/*a*-Si:H systems,[20,69,72,75,81,82] only very few[62,65,70] were taken in a wider temperature range than the 78–300 K range. In many cases the ranges were much narrower than that[83] or were taken above room temperature, providing a very narrow $1/T$ scale.[17,18,28,84]

We start then our consideration of the various scenarios with the non-Arrhenius presentations of the data as manifested, for example, by the many trials to derive the α exponent from the $\sigma_d \propto \exp[-(T_0/T)^{\alpha}]$ dependence that is associated with hopping phenomena.[28,62,69] In particular, we note that the value of α depends on the DOS near the Fermi level, such that if the density of states distribution is given by $g(E) \propto E^s$, where E is the energy of the state, α is given by $(s+1)/(s+4)$.[71] However, for the corresponding dependence over the limited range of temperatures mentioned above it is well known that the distinction between α values in the $1/4 \leq \alpha \leq 1$ interval is very questionable.[36] Moreover, even in the limited ranges that were studied, as are our results in Figs. 6 and 7, *there is no way to fit the data with a single* T_0 value for any α in this regime, in particular for the "popular" $\alpha=\frac{1}{4}$ [variable range hopping (VRH)] or $\alpha=1$ (simply activated transport) values, over the measured temperature range. In fact, as in many other works,[15,17,20,33,78] our presentation of the data with the high and low temperature activation energies is quite artificial since the slope of the Arrhenius plot of our data varies with T. This variation is more likely to indicate some process that varies with temperature than a process that is well characterized by the properties of the system at the extremes of the studied temperature range (that happen to be chosen by the experimental accessibility). It is apparent then that one cannot draw a reliable conclusion as to the nature of the conduction mechanisms solely on the basis of the $\sigma_d(T)$ dependencies. Thus, with no other supporting data, there is no *a priori* justification to present the data by a $\ln \sigma_d \propto T^{-\alpha}$ (with $\alpha \neq 1$) dependence. While the corresponding hopping mechanism is one of the most popular suggestions for the transport mechanism in the μc-Si:H/*a*-Si:H system, the above considerations concerning the value of α, the expectation that these mechanisms are operational only at lower temperatures,[52,66,70,85–87] and the fact that usually it was suggested without specifying the corresponding nature of the states involved cast doubt as to its applicability in one or in all three regimes. In particular, our findings of the similar behaviors shown in Figs. 6(a) and 6(b) and then in Figs. 7(a) and 7(b) are not consistent with the expectations from the suggested VRH-like models (where $\alpha=\frac{1}{4}$ or $\alpha=\frac{1}{2}$). This is mostly since the observation of two regimes in the $\sigma_d(T)$ dependence excludes VRH behavior at the higher (room) temperatures.[88] In particular then, the well-known applicability of the VRH mechanism only to low temperatures in *a*-Si (Refs. 86 and 89) and *a*-Si:H (Ref. 90) and the similarity of our $\sigma_d(T)$ dependencies in all three regimes (phases) suggests that these dependencies are not associated with this mechanism. Also, the values of T_0 that are derived in the literature for the μc-Si:H/*a*-Si:H systems yield rather quite a weak support for the hopping model around room temperature[69] since over the temperature range of the measurement the T_0 values for such data are always of the same order, and thus the use of the, "correct order of magnitude," argument of the density of states (DOS) derived from them is not very convincing. However, noting that at low temperatures the VRH is the only possible transport scenario in disordered systems we will further consider the hopping mechanism in Sec. IV. Of course the E_a values derived from our limited data at low temperatures can be interpreted as representing the transition to a nonactivated process such as intercrystallite tunneling,[65] but again, this regime has not been studied here, and we limited the discussion to our experimentally accessible temperature range (78–300 K).

The other mechanisms that we examine critically, using our above mentioned approach of reducing the number of possible scenarios, are the barrier dependent mechanisms that were suggested for various disordered systems. While the effects of barrier fluctuations[91–93] or an activated tunneling mechanism[94,95] between semiconductor crystallites has not been suggested for the μc-Si:H/*a*-Si:H system, we need, for completeness, to consider the corresponding mechanisms in view of the frequent mentioning[32,68] of various barrier related effects on the transport in this system. However, we do not think that these models apply to our network for the simple reason that *for an a*-Si:H-like phase

no barriers are expected, while the behavior that we observe on our *a*-Si:H-like phase is very similar to the behavior we observed on the phases where crystallites are present and where there may be possible barriers between them (e.g., in the intermediate-x case). Rather, the similar trends that we see in Figs. 6 and 7 for all the x values suggest that the transport mechanisms in all the three x regimes are similar in principle. Hence, we do not present here our $\sigma_d(T)$ data on the various T (non-Arrhenius) scales proposed by the latter mechanisms.

In contrast with the above example of non-Arrhenius presentations one of the most popular mechanisms that was suggested[32,66–68] for the μc-Si:H/*a*-Si:H system and is consistent with the Arrhenius presentation is the thermionic emission model. This mechanism was considered previously mainly for semi-insulating polycrystalline silicon (SIPOS)[96] and polycrystalline silicon (PSi).[97,98] Indeed, *a priori*, the thermionic emission model[97] is consistent with our observations since at low temperatures this emission takes place by tunneling via the lower-energy parts of the barriers while at higher temperature it takes place at the higher-energy parts of the barrier to which the carriers are thermally excited.[96] However, the fact that our results here and results obtained on much smaller or much larger crystallites than ours (20 nm) are similar is in contradiction with the latter model.[97] This is since, as essentially noticed already,[67,99] in the nanoscale there is no meaning to semiconductor depletion regions.[96–98] For example, for semiconductor barriers with the reasonable concentration of donors ($\approx 10^{18}$ cm^{-3}) and a typical density of "surface states" ($\approx 10^{12}$ cm^{-2}) there will be only a couple of electrons (or donors) left (on the average) in a 10–20 nm crystallite. This concentration of carriers or dopants cannot support, of course, such a semiconductorlike barrier. Moreover, under such conditions the observed E_a is known[98] to reveal the energetic separation $E_{Fi}-E_t$ (where E_{Fi} is the intrinsic Fermi level of the crystallite and E_t is the energy of the surface state) rather than some barrier height. Yet, our results for all three μc-Si:H/*a*-Si:H systems, as well as those of others[15,66] for various μc-Si:H/*a*-Si:H systems, in which different size crystallites have been employed, exhibit qualitatively the same ln σ_d vs ln T (concave) behavior and thus are not consistent with the thermionic emission model. In particular, the fact that our results for the *a*-Si:H phase [where no barrier can be expected; Fig. 6(a)] are qualitatively very similar to those of the results in the intermediate phase [where barriers may exist; Fig. 6(b)] further put in question the interpretation of thermionic emission between crystallites in the present system.

Following the above conclusions we turn to suggest the most likely transport and recombination scenarios that emerge from the systematic behavior shown in Figs. 6(a), 6(b), 7(a), and 7(b). We propose that those are consistent with the model of the variation of the equilibrium Fermi level, E_F, within the DOS of a disordered semiconductor in general and in band-tail states in particular.[71,100] In principle, this was the view of Hamasakai *et al.*[101] in their interpretation of the temperature dependence of the conductivity in SIPOS, which followed the band-tail model of Cohen, Fritzsche, and Ovshinsky (CFO).[102] While not as we state explicitly here, various versions of this model have been adopted by quite a few researchers of the μc-Si:H/*a*-Si:H system. However, this was done mainly for the pure μc-Si:H phase which is the most studied phase of the μc-Si:H/*a*-Si:H composite.[52,75,77,78,103,104] In fact, this is not surprising considering the view of ours[37,38] and others[48,66] that for $x>0.7$ the dominant conduction in the system takes place via a disordered Si tissue. This is in particular so considering our finding[37] of band tails in this x regime. In turn, these, as many other works on the high-x regime,[11,20] strongly suggest that a special disordered tissue is responsible for the transport in this regime. Moreover, as suggested above, one can show[64] that in that phase hopping phenomena become significant only at low ($T<50$ K) temperatures. Such a view of conduction in band tails is however much less obvious for the intermediate $0.3<x<0.7$ regime because unlike the above extreme-x regimes, crystallites, as we argued above, are involved in the transport. Indeed as far as we know, this mechanism has not been stated explicitly for the intermediate-x regime. However, in one work for samples with x values in this regime[74] it was suggested that the variation in the values of E_a during the $x\approx 0.3$ transition is associated with the variation of the state distribution in the band gap.

Following the above and our suggestion that the tail state distribution model applies to all the three phases (x regimes), the question that arises is why will the DOS map in all of them be of the same nature in spite of their different structures. We noted already that this scenario is not too surprising for the two extreme-x regimes as it is known to be the case in the low-x (*a*-Si:H-like) regime[71] and since it seems to be quite well established (see the detailed discussion above) for the high-x (columns encapsulating amorphous tissue) regime. The possible answer to that question is then that the crystallite network in the intermediate regime starts to dominate the transport only when the separations between the crystallites in the conduction network are small enough (i.e., of the order of nm; see Fig. 3 and Ref. 17). The barriers act then more like scattering centers than as potential barriers that have to be surmounted.[105] In fact, as we mentioned above in our considerations of the thermionic emission model,[98] the distinction between surface states and bulk states becomes blurred as the crystallites size becomes smaller.

In view of the above, the picture that we suggest is that in all three phases we have a continuous disordered network through which the carriers propagate under the effect of potential fluctuations as outlined theoretically by O'Leary and Lim[106] and that these are manifested by a band-tail state distributions that are reminiscent (but different in their detail) of the CFO model.[102] Of course, the above picture applies also to the $x>x_{c2}$ CETs.[37] We note, however, that for this phase, where crystallites and dopants are present, the gettering of the dopants (intentional, say, phosphorous, or nonintentional, say, oxygen) in the CETs yields a significant increase in the defects in them. In turn, this brings about the corresponding very high carrier concentrations.[61] Indeed this gettering effect explains well the very high conductivity values that are shown in Fig. 6(c) and reported by others[62] that described their results as having a "dirty metal-like" behavior.

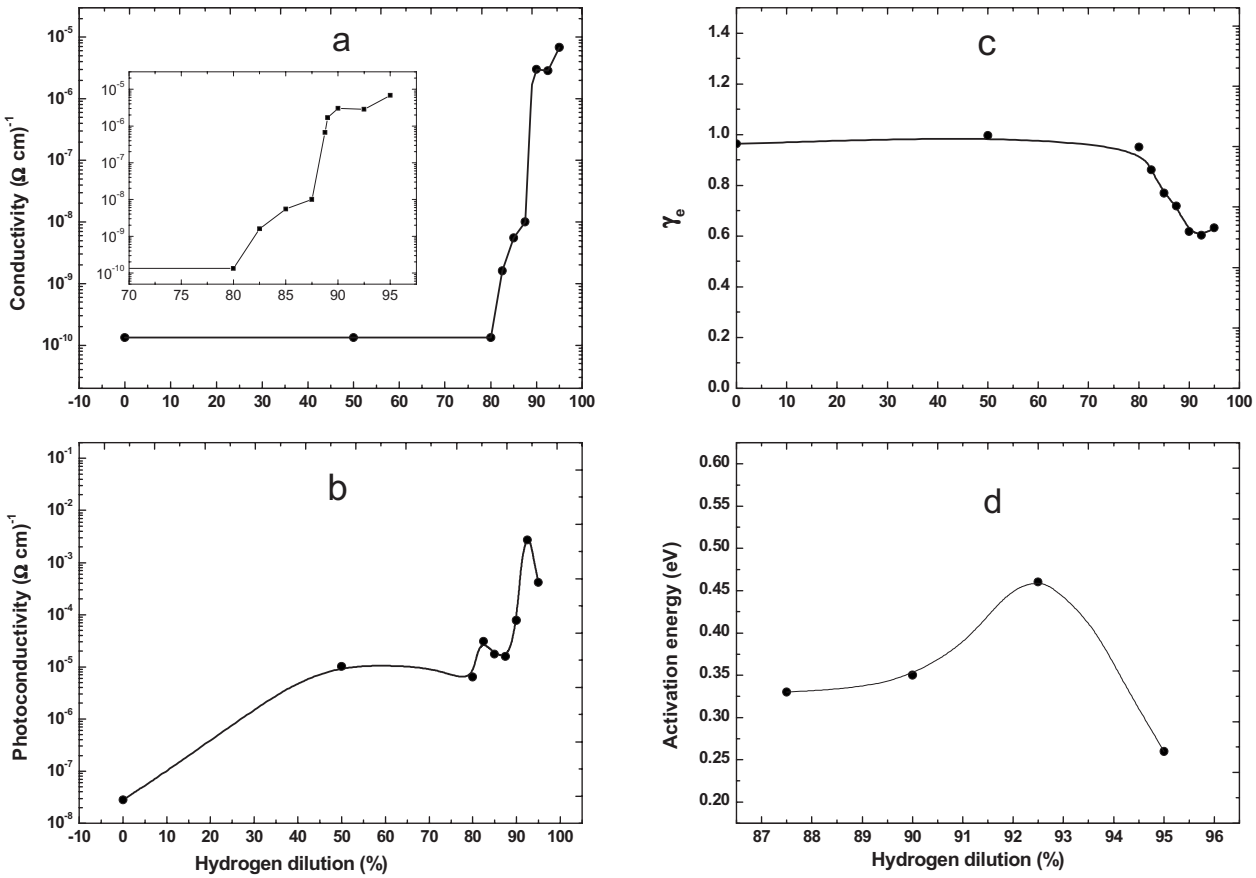

FIG. 8. The dependence of the conductivity, the photoconductivity (for $G=10^{21}$ cm^{-3} s^{-1}), the corresponding light intensity exponent, and the conductivity activation energy on the hydrogen dilution (crystalline phase content) in the undoped samples. Note in particular the typical percolationlike transitions in the more detailed presentatin of the dark conductivity as given in the corresponding inset. The curves are guides to the eyes.

Adopting the above model, we propose then that the activation energy derived at a given temperature, as such, is not very informative, but its value can be considered to reflect (but not necessarily be equal to) the E_c-E_F separation (where E_c is the mobility edge of the conduction band) at a given temperature. Consistent with our results, the effect of doping is then to reduce the E_c-E_F separation for a given landscape of the DOS, on the one hand, and to reduce the E_c-E_{Fq} value (where E_{Fq} is the energy of the quasi Fermi level) upon a given illumination intensity, on the other hand. The latter conclusion is strongly supported by the fact that the $\sigma_{ph}(T)$ dependencies that are found in other disordered semiconductors, in general,[47] and that we[39,60] and others[54] found in the low-x regime, in particular, *are very similar to the ones* shown in Figs. 6 and 7 here.

C. Dependence of the transport and phototransport properties on the concentration of the crystallites

The above discussion concluded that the basic transport mechanism is similar in all the three μc-Si:H/a-Si:H regimes but that there are variations in the landscape of the DOS distribution that yield the different details in the observations. Considering the fact that our main interest in this work is to follow the percolation transitions and to find between what kinds of phases these transitions take place, we turn now to show that, while the basic electronic structure is the same, the electronic properties of the three phases are still quite different since the structural differences that were concluded above are translated into electronic differences between the three phases. This, in turn, will fully confirm that we have two well-defined percolation transitions (between the corresponding three different conducting phases) in the μc-Si:H/a-Si:H system. Following the fact that in the previous literature the transitions observed in the $\sigma_d(x)$ dependence were found in various works at $x\approx 0.3$ and $x\approx 0.7$, we turn to the corresponding dependencies here. These dependencies, for a series of undoped μc-Si:H/a-Si:H samples, are shown in Fig. 8 by providing the full map of the room temperature $\sigma_d(y)$ and $\sigma_{ph}(y)$, as well as the corresponding $\gamma_e(y)$ and $E_a(y)$ behaviors. We recall, of course, that the physically important characterization parameter is the quantity x that scales with the deposition parameter y. In Fig. 8(a) we show the $\sigma_d(y)$ dependence in the entire y range that we studied ($0<y<95\%$), i.e., the entire possible x range ($0\leq x\leq 1$). The "conductivity" for $y\leq 80\%$ reflects the "leakage" resistance of the sample, i.e., our limited experimental resolution. However, recalling that the Raman spectra (Fig. 1) indicate that for the $y<80\%$ range only the a-Si:H phase is detectable, the measured $\sigma_d(y)$ dependence simply

indicates the well-known very high resistivity of this phase, as is the case for pure *a*-Si:H.[71] A clear percolationlike rise[8,45,107] of the conductivity is found then between $y(=y_{c1})=80\%$ ($x_{c1}\approx 0.3$) and $y(=y_{c2})=90\%$ ($x_{c2}\approx 0.7$). At $y=90\%$ we see that there is another abrupt jump in the conductivity. The abruptness of this transition suggests that another percolation transition sets in. However, since unlike the transition at $x\approx 0.3$, the Raman data *do not indicate any particular qualitative changes* of the spectra in the $85\leq y\leq 95\%$ range, it appears then that this conductivity transition is not related simply to the increase of x. Rather, a new x-dependent conducting network, *which is different than that of the randomly distributed crystallites*, is formed around $x_{c2}=0.7$. Recalling that for y at about $y=87.5\%$ ($x\approx 0.5$) the formation of crystallite columns have been suggested[9] and confirmed by the microscopic studies of ours (see above and Ref. 38) and others,[20,49] the simplest interpretation of the macroscopic $\sigma_d(x)$ dependence is that this laterally measured conductivity transition is associated with the formation of a network of these columns. We recall that our structural data showed that it is *not the columns as such* that yield the sharp increase of the conductivity but rather that the increase is related to the percolative *network that consists of a disordered Si tissue* that encapsulates the cylindrical-like columns.

Let us turn now to the phototransport properties considering first the y dependence of the photoconductivity, σ_{ph}, which has hardly been reported before. As shown in Fig. 8(b) this dependence, in the $y>80\%$ regime, follows in its gross features (see, however, below) the behavior of the dark conductivity and in particular it exhibits the presence of two photoconductivity transitions. Considering the fact that the common parameter of σ_d and σ_{ph} is the electron mobility, μ, this behavior primarily suggests that the two transitions in σ_d and in σ_{ph} are associated with the *transport connectivity*, i.e., *with a percolation*, rather than with a change in the carrier concentration (i.e., electronic structure) and/or the recombination (lifetime), mechanism. Noting that in many works only a single transition was observed (see Sec. I) and that no correlated $\sigma_d(x)-\sigma_{ph}(x)$ study was reported, this conclusion is probably the first clear confirmation that the two types of data provide the same self-consistent picture for the presence of three different x regimes in the μc-Si:H/*a*-Si:H system. To further study this point we have examined the dependence of γ_e on y, noting that this parameter is known, as we mentioned in Sec. II, to be *sensitive only to the recombination kinetics*.[47] The results presented in Fig. 8(c) show that γ_e is constant for the entire $y<80\%$ ($x<0.3$) regime, suggesting that no variation in the recombination mechanism takes place in this interval, i.e., that in this regime the phototransport is associated with the *a*-Si:H-like phase. Then, the combined local decrease of $\mu\tau_e$ and γ_e in the intermediate y regime ($0.3<x<0.7$) suggests the appearance of a new recombination mechanism, i.e., with the recombination in the crystallite-percolation network that dominates the photoconduction in the intermediate phase of the μc-Si:H/*a*-Si:H system. This view follows the suggestion[34] that the photogenerated carriers that contribute to the conduction are only those that are generated in the backbone of the corresponding percolation network, i.e., in the network that consists of very close crystallites (see Sec. III B). In turn, this suggestion supports our above view that the intermediate regime here is similar to the one encountered in granular metal networks above the percolation threshold.

Considering the other phases we note that in the *a*-Si:H-like phase ($0<y<80\%$) there is a small increase of the photoconductivity, i.e., in the value of $\mu\tau_e$. This behavior is consistent with the suggestion[108] that under the conditions that bring about the formation of microcrystallites some local structural changes (that are manifested by a change in the concentration of the dangling bonds[60]) take place in the *a*-Si:H phase. In the higher $y-(x>0.7)$ regime, the increase of γ_e indicates again that a change in the recombination mechanism takes place. In particular, we see that the overall $\gamma_e(y)$ behavior suggests that the recombination process in the intermediate-x regime is different than those of the *a*-Si:H-like[39] and the disordered CET[37] regimes that we studied in detail previously. In turn this finding strongly supports our view that the main differences in the recombination mechanisms between the three phases are due to the differences in the state distribution profiles of their band tails. Let us add in passing that the phototransport properties of the minority carriers[37,39] (that will not be discussed here) have indicated correlated variations in the phototransport mechanism in the three regimes. Of course, we should emphasize that the recombination related variations with x are quite subtle compared to the variations of the electron "mobility-connectivity" variations that are manifested by the relatively large variations of σ_d and σ_{ph} at the two percolation transitions.

Confirming the generality of our observed $\sigma_{ph}(y)$ dependence and considering its difference from the $\sigma_d(y)$ dependence in its detail, we concluded that there is a clear indication that the conductivity transitions do not reflect only variations in the mobility-connectivity mechanisms but that they also *reflect differences in the recombination mechanism in the three different x* regimes. In contrast, the differences in the transport mechanisms in the three phases are not as conclusive in the case of the undoped samples, as can be seen from the $E_a(y)$ dependence. This is since, as shown in Fig. 8(d), we have very few data (as emphasized by the corresponding expanded y scale) for this parameter. The observed variation in the values of E_a in the intermediate and high-x regimes will be further discussed below.

As pointed out above, in order to be able to measure the macroscopic transport properties at lower temperatures and in the low-x regime, we had to perform measurements on doped μc-Si:H/*a*-Si:H systems. A summary of the macroscopic data that were obtained on the doped samples is shown in Fig. 9. As for the results shown above for the undoped samples we can clearly distinguish in Fig. 9 between the two transitions and conclude from the observed similar jumps of the conductivity and photoconductivity, in Figs. 9(a) and 9(b), that these are associated primarily with mobility-connectivity transitions. Also, as above, the most informative parameter that can be derived from the $\sigma_d(T)$ dependence is E_a. Correspondingly, as noted above, while the actual E_a values are not too informative as such, their trends of increasing with temperature and decreasing with subsequent percolation transitions are informative. This behavior, being much clearer than in the undoped samples, in-

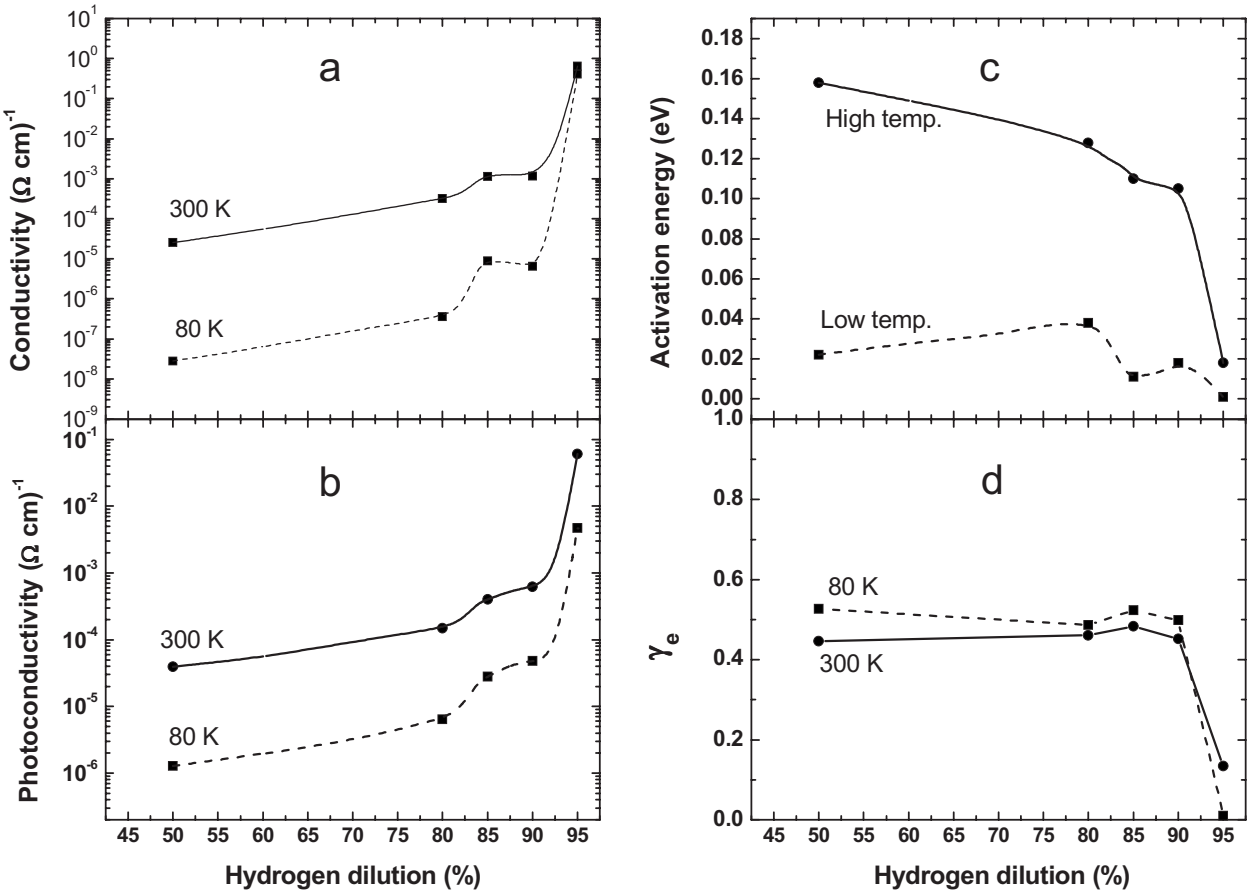

FIG. 9. The dependence of the conductivity, the photoconductivity (for $G=10^{21}$ cm^{-3} s^{-1}), the activation energy, and the corresponding light intensity exponent on the hydrogen dilution (crystalline phase content) in the doped samples. The curves are guides to the eyes.

dicates then again that a different conducting phase is dominant in each of the three regimes that are separated by the two percolation transitions.

The relatively modest jumps in $\sigma_d(y)$ and $\sigma_{ph}(y)$ for the low x ($x_{c1} \approx 0.3$) transition in Fig. 9 seem to justify the EM approach[3,107] proposed previously[27,33] and our above corresponding assumption that in the intermediate-x regime the crystallites form the dominant conducting percolative network. Two competing effects can be considered here. On one hand, the doping of the crystallites is ~100 times more efficient than that of a-Si:H, and on the other hand, the crystallites form a much more tortuous current percolation network in comparison with the continuous matrix of the doped a-Si:H phase. Returning to the E_a values in Fig. 9(c), which we derived in the low temperature (80–100 K) and the high temperature (200–300 K) ranges for the intermediate $80 < y < 90\%$ regime, we see that the low temperature activation energies of σ_d are less than about 0.04 eV while in the high temperature range the activation energy E_a is found to vary between 0.16 and 0.10 eV. The clear transition here in the E_a values at $y=80\%$ correlates well with the transitions we saw in Fig. 8, yielding now a more convincing indirect evidence for a formation of a conducting route of microcrystallites within the intermediate-x regime. The fact that a similar transition is also observed for the low temperature data is quite a clear indication that the reason for the transition is due to the variation in the connectivity (i.e., in the percolation) of the system. In turn, this may also suggest that there is no variation in the transport mechanism within the studied temperature range. The photoconductivity data that we show in Figs. 9(b) and 9(d) reaffirm even more clearly our above evaluation for the two transitions in the transport and recombination mechanisms as x is varied, emphasizing that these are simultaneous and thus suggesting that both are also associated with the differences in the DOS distributions in the three phases. In particular, the drastic drop in the γ_e values in the $x>0.7$ regime confirms that the doping does not enable the shift of E_{Fq} with G and then, that there is a drastic decrease of τ_e that competes with the strong increase in μ. This competition appears to yield then the resultant behavior shown in Fig. 9(b) for this regime. In a way, this strong enhancement of the carriers' recombination further justifies the application of the above mentioned concept of dirty metal[62] that was used to describe the heavily doped high-x phase.

While we were concerned in Fig. 9(d) above only with demonstrating that significant changes in γ_e take place at the percolation transition (without being concerned with the very specific recombination mechanism) it is worth noting in passing that the sub-$\frac{1}{2}$ values of γ_e should not be considered as unusual or surprising as one may conclude from the classical literature.[47] Such sub-$\frac{1}{2}$ values have been obtained by many authors on various photoconductors. In fact, we have obtained such results experimentally not only on undoped

a-Si:H (Ref. 39) and undoped μc-Si:H (Ref. 37) but also on $CuInSe_2$ and CdTe systems. Extensive simulations (such as in Ref. 39) have shown that these values are associated with sensitization effects[47] that are effective when the resultant recombination is determined by the two types of carriers and by more than one set of recombination centers. So far however, no such simulation has been carried out for doped μc-Si:H. One further notes that for the latter system [i.e., the one considered in Fig. 9(d)] the situation is much more complicated then in the undoped case [that is considered in Fig. 8(c) and Ref. 37] since in addition to the band tails and dangling bonds it includes the dopant states as well as the many "free" carries.

D. Special importance of the oxygen doping in the high concentration regime

Before the conclusion of the presentation of our results let us try to account for the difference found between our C-AFM results and those reported by Rezek *et al.*[50] for the high-x $(0.7<x<1)$ regime. While the AFM topography of the samples in their works is very similar to that of ours, their C-AFM results show that the conductance via the individual crystallites within the columns is higher than via the CET. This observation is in contrast with previous results of ours[38] and others,[49] as well as the results that are shown in Fig. 5 here. Following the precautions that we took, as mentioned in Sec. III A, it appears to us that a possible clue for this discrepancy is provided by the fact that the currents that they observed via the crystallites were of the order of 1 pA. This is also the current that we observed via the crystallites but, in our study, these weak currents come only as additions to the much larger currents via the disordered CET (see Fig. 5). This suggests that there is a basic difference between their samples and our samples. Noting in particular that their samples were deposited (by a different deposition technique) and tested in ultrahigh vacuum further suggests that the oxygen content in our samples is much higher than in theirs (see Sec. II above). We attribute this difference (as discussed in more detail in Sec. IV) to the fact that [similar to *a*-Si:H (Refs. 109 and 110)] the oxygen "doping" of μc-Si:H, as $x\rightarrow 1$, is very efficient,[111–113] on the one hand, and to the fact that the corresponding dopants substantially increase the conductivity of this system,[84,111,113,114] on the other hand.

In order to further test this suggestion (and being aware of the more than 10^{18} cm^{-3} oxygen atoms in our samples) we conducted a scanning tunneling spectroscopy (STS) study[51] on our μc-Si:H/*a*-Si:H doped and undoped samples. One of the current-voltage (*I-V*) characteristics taken on an undoped $x\approx 1$ sample is shown in Fig. 10. The *I-V*, and more clearly the $dI/dV-V$ characteristics reveal a peak in the DOS at an energy level, E^*, which lies 0.3–0.4 eV above the valence-band edge, E_v, and 1.1 eV below the Fermi level, E_F. On the other hand we see from these results that $E_c-E_F\approx 0.2$ eV. This is in excellent agreement with our above assumption that $E_a\approx E_c-E_F$ considering our observation that the E_a values for the undoped samples are in the 0.2–0.3 eV range. We can conclude then a band gap that is within the range of 1.6 and 1.8 eV. The fact that such an optical (Tauc) band gap

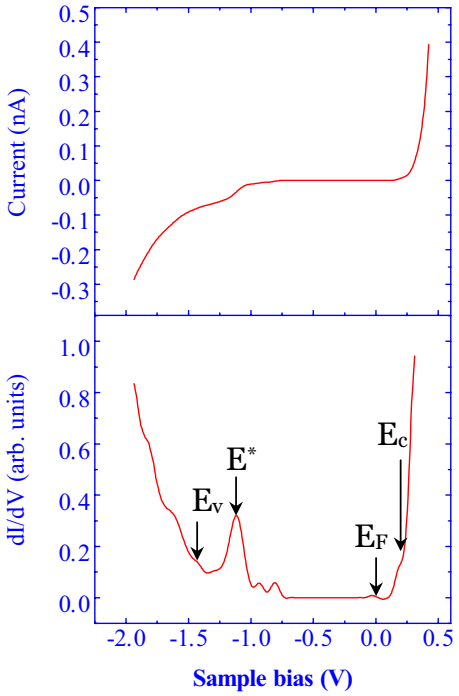

FIG. 10. (Color online) *I-V* and $dI/dV-V$ tunneling characteristics that were measured on a pure (undoped) μc-Si:H sample. The Fermi level, E_F, the conduction and valence-band edges, E_c and E_v, and the energy of the involved states, E^* (as suggested by the latter spectrum for this *n* type but nonintentionally doped material), are indicated in the figure.

exists in this phase[115] strongly supports this DOS distribution interpretation of the STS result that we show in Fig. 10. This interpretation is also in excellent agreement with our previous conclusion from very different considerations[39] regarding the existence of a "level" or a peak in the DOS, which lies 0.3–0.5 eV above E_v, in our *a*-Si:H samples (that were prepared under similar conditions to the samples used in the present study). We suggested then[39] that this level is associated with the known presence of oxygen in *a*-Si:H. In fact our STS data are probably the direct proof for the safe hole-trap level in the μc-Si:H/*a*-Si:H systems, as has been suggested many years ago[116] for *a*-Si:H. This is since the present finding enables us to confirm the correlation between "safe" (high cross section) hole traps and oxygen associated defects as suggested by us[39] and by others[117,118] who arrived at the same conclusion following other types of indirect measurements. Moreover, our association of the observed hole traps with the high oxygen content in our samples is also well supported by the fact that hole traps are known[119] to exist in defective silicon oxide. Following these observations it appears then that the involvement of the oxygen induced states yields, as suggested for *a*-Si:H,[117] carrier donating states on the one hand and acceptorlike defects, close to the valence-band edge,[37] on the other hand. This is then apparently the reason for the high local and global conductivity of the disordered CETs.

IV. SUMMARY AND DISCUSSION

In this paper we reported a comprehensive-systematic study of percolation transitions and their corresponding

phases in a semiconductor composite. Our study has shown that indeed an *a priori* two-phase semiconductor composite is a more complicated system than the traditional two-phase systems that were treated by the effective medium (EM)[3,33] or interparticle tunneling-only theories.[45,120] Rather, interfaces between "phases" play a very special role in the macroscopic transport behavior of the above systems. We have further shown that this complexity does not enable, *a priori*, to correlate the macroscopic behavior with the simple nominal composition of the constituents in such systems. This is in sharp contrast with the more common percolation systems such as the metal-insulator composites of granular metals[45] and carbon particle-polymer composites.[2,120] Hence, following the present study it appears quite conclusive that in order *to evaluate the transport mechanisms in semiconductor composites a simultaneous study of the microscopic routes and the corresponding macroscopic behavior of the transport is essential*. In particular, we concluded that the macroscopic characterizations of the structure, as for example by Raman scattering (e.g., crystallinelike features that are observed), are not enough to reveal the nature of the conducting network since the same particles can be assembled in different configurations. Also, the application of local spectroscopy is found to be very helpful in the determination of the finer details of the nature of the conducting phases and the transport and recombination mechanisms that accompany the various current routes.

Turning to the evaluation of the transport routes and mechanisms in the μc-Si:H/a-Si:H system that we have chosen here as a prototype of a semiconductor composite, we have reached the following conclusions. Starting from the percolation transitions, we have established beyond any doubt that there are two clear macroscopically observable percolation transitions, which are *common to both doped and undoped samples*. Using a combined Raman and local transport microscopy studies we have found that while the $x \approx 0.7$ transition is very clearly associated with the onset of intercolumnar connectivity, the nature of the $x \approx 0.3$ transition that is associated with the formation of crystallites is less apparent. In the latter case two types of transitions are possible in principle. In one, the conduction above the percolation transition is expected to be by tunneling between the crystallites, as in the tunneling-percolation transition[2,45] (such as we observed in granular metals in the so-called dielectric regime, with a threshold at 18 vol % of the metal content[120]). In the other, which is much better known (with a typical threshold at about 50 vol % of the metal content[4,120]), the conduction is associated with a network of coalescing grains. We found that in the system studied here there is supporting evidence only for the second type of transition in the $x \approx 0.3$ case (the higher metal vol % transition in granular metals) except that instead of a coalescence of the metallic grains we have a very close contact between the crystallites. This follows, apparently, from the fact that in the μc-Si:H/a-Si:H system, only when the network of crystallites has a backbone that is made of crystallites separated from each other by no more than about 1 nm (see, e.g., Fig. 3 and Refs. 17 and 121), it can compete with the conduction via the noninsulating a-Si:H embedding matrix. This view is supported by the a-Si:H-like behavior in the $x < 0.3$ regime (that was observed and questioned but not explained[11,54]) as well as the higher carrier generation rate in the crystallites, which was observed and explained[34] for the $x > 0.3$ regime (where the two phases are detectable).

Identifying the two percolation transitions in the μc-Si:H/a-Si:H system we expected that three separate, electronically different, phases can be identified and characterized by their macroscopic properties. Correspondingly, we performed a detailed analysis of the macroscopic transport and phototransport properties from which we have established that qualitatively similar, but quantitatively very different, conduction mechanisms are involved in the three types of current networks that are associated with the three different phases (the $x < 0.3$, $0.3 < x \leq 0.7$, and $0.7 \leq x \leq 1$ regimes). While we were able to reveal only the gross framework of the electronic properties of the three phases associated with the three current networks, this was enough to demonstrate that they are different, leaving the more exact nature of the corresponding transport and recombination mechanisms to later studies.

In what follows we will try to show that the conclusions that we derived here are consistent with many of the data in the literature *when these data are considered within the context of their appropriate* x values. In particular, we will try to show that a particular intermediate-x phase does exist in the μc-Si:H/a-Si:H system. This is to be contrasted with the fact that all previous works that have observed the $x \approx 0.3$ transition (see Sec. I) did not characterize this regime and thus did not confirm nor even suggested that such an electronically distinguishable intermediate phase exists. Importantly, our identification of the intermediate phase gives us, in turn, the ability to construct the framework for the discussion of the entire μc-Si:H/a-Si:H system. This framework will enable us to determine the transport mechanisms, on one hand, and to resolve the long standing and thus far unresolved question[11] of why there is a similarity between the transport and recombination properties in the various μc-Si:H/a-Si:H systems and in the a-Si:H system, on the other hand.

Our main tool for the evaluation of the transport mechanism was here the temperature dependencies of the conductivity and photoconductivity. In our analysis of the observed $\sigma_d(T)$ and $\sigma_{ph}(T)$ characteristics we have chosen to present the data by Arrhenius plots rather than other possible presentations that are associated with some other specific mechanisms. The fact that all our data for the entire-x range, when presented on a $\ln \sigma$ vs $\ln T$ scale, yield a concave dependence suggests some basic similarity of the three phases in the system. This suggestion becomes very convincing when one notes that in many other studies on μc-Si:H/a-Si:H systems[15,32,56,65,79] and related disordered,[122] nanocrystalline,[17] amorphous,[58,123] and hydrogenated amorphous[21,63,90] silicon systems, such a concave behavior was found. One should further note that the μc-Si:H/a-Si:H composite is quite similar to SIPOS and PSi for which such results[92,105] were interpreted[101] as due to the variation of the Fermi level position within the density of states landscape (that is CFO-like[88,102]) when the temperature is varied. Adopting the basics of this model to the system studied here (see Sec. III B) we note that this model is very different from

the thermionic emission[15,29,67] or other barrier limited transport[23,30,65,76,124,125] models that were suggested by many authors to describe the transport process in the various μc-Si:H/a-Si:H systems. The main reason for the conclusion that the barrier-based models do not apply to the present system is that, as mentioned above, the observed dependencies of $\sigma_d(T)$ and $\sigma_{ph}(T)$ are very similar to those observed not only in various microcrystalline and nanocrystalline Si materials but also in a-Si:H (Refs. 90 and 126) where there *are no apparent barriers in the system*. There is also ample evidence against the role of the barriers as such, as manifested by the estimations of their small heights[121,127] and small widths[17,128] in various μc-Si:H/a-Si:H systems.

Following our above model of transport in band tails our view is then that when crystallites are present, the narrow separation between two adjacent crystallites acts "only" as a local disturbance in the potential landscape over distances such as those encountered in amorphous semiconductors[106] (though at a smaller spatial "frequency" that is mainly determined by the crystallites size). This picture is also consistent with the, macroscopically found, relatively high mobility values reported for the μc-Si:H/a-Si:H systems[53,76,121,128,129] in general and for the intermediate-x regime in particular. The relatively large mobility values indicate then that the above potential fluctuations act as carrier scatterers.[105] The fact that band-tail state distributions are found even in PSi where the crystallites are usually larger[130,131] further supports this view. Another strong support to this view comes from the similarity of the photoconductivity behavior found here in all the three ($y=50\%$, 87.5%, and 95%) regimes[34,37,39,54] and its similarity with the observations on a-Si,[132] a-Si:H,[57,59,60] and chalcogenides.[47] In fact this further suggests that, as in the latter systems, the conduction in the μc-Si:H/a-Si:H system takes place in extended states that are associated with a *continuous network of a disordered semiconductor*. In passing we note (see also below) that the scenario that we ascribe here is similar to the one suggested[133–135] for many of the polycrystalline silicon systems. Similarly, as well confirmed by the variation of γ_e that we found here, the recombination mechanism varies as the band-tail map varies from that of a-Si:H (Refs. 39, 71, 86, and 136) to that of the intermediate phase[73,74] and then to that of the CET,[11,37,64,70,103] as x increases.

Examining the literature one finds ample supporting evidence for the picture that we tried to describe above. For brevity we will mention here only few of them. In some works, the height of the intercrystallite barrier and its effect on the transport were found to be negligible.[76,99,137] In other works, the variation of $E_a(T)$ with temperature has been concluded to be associated with the shift of E_F in the band tails.[18,74–78] Correspondingly and following the phototransport data, the view of carrier conduction in a homogeneous disordered network has been proposed.[43,64,77] The transport and the phototransport are dominated then by a continuous disordered "tissue"[37,64] that structurally and electronically is reminiscent of a-Si:H but, as we have shown previously, different in detail from it.[37] This situation is expected to become less and less likely, and the concentration of the tail states will decrease, as the crystallites size increases to become of the order of 100 nm. Indeed in polycrystalline silicon the density of states is also found to be "made" of band tails[130,131,133] but the carrier mobility is larger than that of the μc-Si:H/a-Si:H composites.

Assuming the presence of band tails in all the above mentioned systems, the transport is expected to take place at very low temperatures, by hopping, and at higher temperatures in extended states.[11] Of course, the transition temperature between the two ranges of temperature will shift to lower temperatures as we go from the a-Si:H phase[126] to the polycrystalline phase.[135] Generalizing our model then we even suggest that on passing from a-Si:H to polycrystalline silicon it is the potential fluctuations in the systems that determine the band-tail state distribution in them and thus the corresponding transport and recombination mechanisms. In particular, this includes the three μc-Si:H/a-Si:H phases. We expect of course, as indeed turned out to be the case, that the heights and the widths of the tails will be reduced on passing from a-Si:H to PSi via the μc-Si:H/a-Si:H systems. However, the gettering effects[61,114,138] and the fact that the columnar tissue is a disordered system appear to suggest that of the three phases the band tails will be the least pronounced in the intermediate-x regime. We note that, indeed, while there are ample evidences of band-tail state distributions in the extreme-x regimes[37,39] there are only very few works that suggest the existence of band tails in this intermediate regime[55] that consists of "almost coalescing"[134] crystallites.

That our present work and our above conclusions do indeed set now the framework for the understanding of the μc-Si:H/a-Si:H systems is exemplified by some issues that were unresolved in previous studies. Starting with the percolation transition as such, we note that in contrast with the works in which the percolation transitions were found to be blurred,[12] the present work shows clearly that the $\sigma_d(x)$ dependence consists of two "sharp" separate percolation transitions and that the two transitions are of a very different origin. Moreover, the fact that the $x \approx 0.7$ transition has not been previously reported[20] for doped samples could have been explained as due to doping induced variations in the structure or in the basic electronic structure of the corresponding system. Our present results on doped and undoped samples indicate that the two percolation transitions take place at the above x values in the two types of samples. The fact that these values are equal to those observed in some doped ($x \approx 0.3$) and some undoped ($x \approx 0.7$) systems in the literature provides *a posteriori* evidence that the two (doped and undoped) types of systems are structurally the same. The only differences are, as in crystalline semiconductors, manifested in the quantitative behavior of the electronic properties. Hence, the comparison we made between all the data is well based.

The above "semiconductorlike" behavior can also explain the photoconductivity dip that appears to be associated (here and, e.g., in Ref. 26) with the intermediate-x regime. While the $\sigma_d(x)$ dependence represents mainly the mobility and connectivity aspect of the system, the $\sigma_{ph}(x)$ represents also the recombination mechanism (i.e., τ). Thus, a decrease in σ_{ph} ($\propto \mu\tau$) is not unexpected. Then, of course, as x further increases, the percolation route of the CETs sets in and both the conductivity and photoconductivity have their relatively strong rise.

A major issue arises when one compares our previous[38] and present C-AFM conclusions with those of Rezek *et al.*[50] for the $x>0.7$ regime. They suggested[20] that the local currents take place through the crystallites within the columns and thus, that a semiconductor, bandlike, conduction prevails. On the other hand, in contrast to this, they interpreted their macroscopic transport measurements, on samples that were exposed to the ambient atmosphere, as indicating conduction in a silicon disordered phase rather than a band conduction via crystallites.[103] Considering this and the precautions that we took in our work, we interpreted, in Sec. III D, the differences between our results and theirs as due to the different types of samples used in the two studies. In particular, following the expected exposure and the sensitivity of the CETs to ambient gases[114,138,139] it appears that the difference between the two types of samples is associated with the very different oxygen content in the CETs of our samples in comparison with that of theirs. We conclude then, based on our findings and additional findings in the literature,[48,112] that the oxygen doping and the gettering effect[61,114] make the CETs to be the major current conducting route in the high-x regime and, thus, that both the transport and the recombination mechanisms that we observed are attributed to the disordered CETs.

Another issue associated with the interpretation of the conduction via the CETs is the percolation threshold at $x\approx 0.7$ which "*a priori*" was suggested to be associated with a simple system of randomly placed but closely packed parallel cylinders and thus a surface (cross section) coverage of 44% was expected.[140] This, however, (as seen in Figs. 4 and 5) is not consistent with our findings here. To reliably address this problem one must note that the common Scher-Zallen approach, usually cited in similar contexts, is not appropriate for the present system since there are no "insulating spacers" here of the size of the columns, such as in the two-dimensional Scher-Zallen disk model.[2] Rather, a much more dense packing, as concluded by us qualitatively[141] and by others quantitatively,[142] is expected to yield that the value of x_{c2} should be within the $0.5<x_{c2}<0.8$ interval. This prediction is then in excellent agreement with our present evaluation of the $x_{c2}\approx 0.7$ transition. Moreover, as can be found by comparing our AFM and C-AFM images for a dilute system of columns[38] with our present images for the densely packed columns (Figs. 4 and 5), the cross section of the columns has a form of a polygon rather than being circular. Indeed, the packing of the plane by polygons (say, hexagons) is much denser than that of circles and thus the much higher packing density. In turn, this means that the columns touch *each other not by a line* (*or an edge*) *but by joint planes*. This realization is important for the present interpretation of the transport in the high-x phase since (in addition to the oxygen doping and the other impurity gettering effect) it accounts for the high connectivity of this phase and explains well the very high conductivity and the very high recombination rate that we observed for the undoped as well as for the corresponding doped [with a conductivity of the order of 1 $(\Omega\,\mathrm{cm})^{-1}$] samples. That the columns always contribute significantly in the vertical configuration is apparent from our previous work,[38] while here we demonstrated that only as x becomes larger than 0.7 we get the CET network to contribute significantly to the lateral-percolation conductivity. Of course, the above considerations explain also the well-known anisotropy reported for the transport and phototransport properties of the μc-Si:H/a-Si:H systems.[20] It is clear now that this anisotropy is associated with the degree of participation of the columns in the transport. The conduction by the individual columns increases with x already in the intermediate-x regime, but this contribution is manifested only in the vertical configuration. In contrast, in the high-x regime, the columns (or rather their CETs) contribute to the transport in both the vertical and the lateral configurations. We note in passing that the idea that the above anisotropy is associated with the formation of columns has been suggested before,[20,48,143] but the variation of the transport and recombination mechanisms, at the onset of the corresponding lateral-percolation transition, has not been discussed. We also note that a similar but a three-dimensional Scher-Zallen argument was suggested[144] for the low $x\approx 0.3$ transition. However, again, the lack of spherical "spacers" renders this model inappropriate for the present system. Rather, the granular metals[4] or EM models[33] for the formation of a continuous network[4,120] are more applicable to this case that, as we have concluded from other considerations, yield a threshold value at $x\approx 0.3$.

Turning to the summary of this work we start with the general achievements of the present study regarding the transport, the recombination, and the percolation mechanisms in the μc-Si:H/a-Si:H system. Considering our previous[37–39] and present results, as well as conspicuous reports in the literature by others, we were able to show that one of the previously suggested mechanisms is more credible than others and to show that the three phases that are determined by the two percolation transitions can be well distinguished from each other while being controlled by, basically, the same transport and recombination mechanisms. The other conclusions were that the transition between the low-x and the intermediate-x phases is the semiconductor equivalent of the percolation transition in granular metals, while the transition from the intermediate-x phase to the high-x phase is a transition that is quite unique to semiconductor systems. Beyond the above broad picture we have determined the more specific transport and recombination mechanisms in each of the three phases as follows.

The basic picture that we concluded here for the $x<0.3$ phase is that, while crystallites are present in it, they or their clusters are not electrically connected to the degree that their contribution to the transport can compete with the a-Si:H matrix. On the other hand, the conditions under which these samples are prepared[60,108] yield that the a-Si:H-like phase is of comparatively low concentration of dangling bonds and thus the transport and the recombination mechanisms are dominated by the a-Si:H-like band tails. Hence, we conclude the dominance of the E_F shift at high temperatures[71] and the dominance of hopping only at low temperatures.[64,88]

At the other end, i.e., that of the high-x phase, we found that the electronic structure of the silicon disordered tissue that encapsulates the existing columns of crystallites consists of two band tails.[37] The conduction-band tail was shown then to be similar to that of a-Si:H while the valence-band tail was shown then to be very different from that of a-Si:H. The carrier recombination is controlled however by the valence-

band-tail states throughout the entire temperature range. Turning to the conduction mechanism we note that while this has not been suggested explicitly previously, the conduction via band-tail states has been concluded indirectly[64] from photoconductivity data that are similar to those of ours. Hence, at low temperature the conduction mechanism is by hopping (rather than by variable range hopping[28]) via the transporting level[87,100] in band-tail states. At high temperatures, as for disordered semiconductors, the conduction is concluded here to be carried via extended band-tail states.

The intermediate-x regime, which consists of x values in the interval $0.3 \leq x \leq 0.7$, has hardly been discussed previously as such, although many data have been accumulated for it. In fact almost all possible transport mechanisms have been proposed for this regime and most of them (as in the high-x regime) were suggested to be associated with transport involving effects of barriers or energy level separations between two adjacent crystallites. In view of the fact that the two coexisting phases (the crystallites and a-Si:H matrix) may contribute almost equally to the conductance in this regime, it is not surprising that in some works a-Si:H-like behavior has been attributed to this regime[54] while in others the very different transport mechanism of granular metals below the percolation threshold[17] was proposed. In our view, however, the higher conductivity here, compared to that of the $x < 0.3$ regime, indicates that the dominant conduction is via the network of the crystallites that are embedded in the a-Si:H matrix. This network is similar to that of the metallic (particle coalescence) regime in granular metals[4] (and not with the percolation-tunneling model[107,120] that does not assume coalescencelike contacts between the conducting particles). We further concluded that the interfaces between the crystallites provide "minor" (low and narrow) potential barriers that act more like scattering centers than barriers.[127] Hence, they yield potential fluctuations, such as defects in crystals or imperfections in disordered semiconductors, thus bringing about the above discussed band tails in the system.

In conclusion, by combining microscopic and macroscopic studies, we have shown that very different three types of transport routes, but not too different transport and recombination mechanisms, are exhibited when the density of the microcrystallites increases in the μc-Si:H/a-Si:H composite system. The three regimes that evolve with the increase of this density are marked by two percolation transitions which are of very different nature. The lower density one is of a three-dimensional nature, while the higher density one is of a two-dimensional nature. The transport and recombination mechanisms for all three phases are controlled by the band tails in them. The differences in the corresponding types and distributions of the states in the tails account for the observed differences in the macroscopic transport and recombination properties as well as for the percolation transitions that are observed in the μc-Si:H/a-Si:H system.

ACKNOWLEDGMENTS

The authors are indebted to Y. Goldstein for many helpful discussions. This work was supported in part by the Israel Science Foundation (ISF) and in part by the German Federal Ministry of Environment, Nature Conservation and Nuclear Safety (BMU). I.B. acknowledges the support of the Enrique Berman chair of Solar Energy Research at the HU and O.M. acknowledges the support of the Harry De Jur chair of Applied Science at the HU.

[1] D. Stauffer and A. Aharony, *Introduction to Percolation Theory* (Taylor & Francis, London, 1994).
[2] I. Balberg, in *Percolation*, Springer Encyclopedia of Complexity Vol. 2, edited by M. Sahimi and R. A. Myers (Springer, Berlin, 2009), p. 1143.
[3] R. Landauer, J. Appl. Phys. **23**, 779 (1952).
[4] For reviews see B. Abeles, Appl. Solid State Sci. **6**, 1 (1976).
[5] P. Sheng, Philos. Mag. B **65**, 357 (1992).
[6] See, for example, J. M. Benoit, B. Corraze, and O. Chauvet, Phys. Rev. B **65**, 241405 (2002).
[7] For a review see O. Bisi, S. Ossicini, and L. Pavesi, Surf. Sci. Rep. **38**, 1 (2000).
[8] I. Balberg, E. Savir, J. Jedrzejewski, A. G. Nassiopoulou, and S. Gardelis, Phys. Rev. B **75**, 153301 (2007).
[9] L. Houben, M. Luysberg, P. Hapke, F. Carius, F. Finger, and H. Wagner, Philos. Mag. A **77**, 1447 (1998), and references therein.
[10] For a review see R. E. I. Schropp and M. Zener, *Amorphous and Microcrystalline Solar Cells, Materials and Device Technology* (Kluwer, Boston, 1998).
[11] For a recent review see W. Fuhs, J. Non-Cryst. Solids **354**, 2067 (2008).
[12] S. Koynov, S. Grebner, P. Radojkovic, E. Hartmann, R. Schwarz, L. Vasilev, R. Kronkenhagen, I. Siebec, W. Hernion, and M. Schmidt, J. Non-Cryst. Solids **198-200**, 1012 (1996).
[13] T. Kamei, P. Stradins, and A. Matsuda, Appl. Phys. Lett. **74**, 1707 (1999).
[14] K. Shimakawa, J. Non-Cryst. Solids **266-269**, 223 (2000).
[15] F. Liu, M. Zhu, Y. Feng, Y. Han, J. Liu, S. Kasouit, and R. Vanderhaghen, J. Non-Cryst. Solids **299-302**, 385 (2002).
[16] V. G. Golubev, V. Y. Davidov, A. Medvedev, A. B. Pevtsov, and N. A. Feoktisov, Phys. Solid State **39**, 1197 (1997); A. B. Pevtsov, V. Y. Davidov, N. A. Feoktisov, and V. G. Karpov, Phys. Rev. B **52**, 955 (1995).
[17] Y. He, Y. Wei, C. Zheng, M. Yu, and M. Liu, J. Appl. Phys. **82**, 3408 (1997), and references therein.
[18] D. Han, G. Yue, J. D. Lorentzen, J. Lin, H. Habuchi, and Q. Wang, J. Appl. Phys. **87**, 1822 (2000).
[19] A. L. B. Neto, A. Lambertz, R. Carius, and F. Finger, J. Non-Cryst. Solids **299-302**, 274 (2002).
[20] J. Kocka, A. Fejfar, H. Stuchlikova, J. Stuchlik, P. Fojlik, T. Mates, B. Rezek, K. Luberova, V. Suncek, and I. Pelant, Sol. Energy Mater. Sol. Cells **78**, 493 (2003), and references therein.
[21] N. Pinto, M. Ficcadenti, L. Morresi, R. Murri, G. Ambrosone, and U. Coscia, J. Appl. Phys. **96**, 7306 (2004).
[22] J. Kocka, T. Mates, H. S. Stuchlikova, J. Stuchlik, and A. Fejfar, Thin Solid Films **501**, 107 (2006).
[23] H. Overhof, M. Ott, M. Schmidtke, U. Backhusen, and R. Carius, J. Non-Cryst. Solids **227-230**, 992 (1998).

[24] P. Alpuim, V. Chu, and J. P. Conde, J. Appl. Phys. **86**, 3812 (1999), and references therein.
[25] M. Jana and D. Das, Sol. Energy Mater. Sol. Cells **79**, 519 (2003).
[26] S. Koynov, R. Schwarz, T. Fisher, S. Grebner, and H. Munder, Jpn. J. Appl. Phys., Part 1 **33**, 4534 (1994).
[27] R. Carius, F. Finger, U. Baehausen, M. Luysberg, P. Hapke, L. Houben, M. Otte, and H. Overhof, *Amorphous and Microcrystalline Silicon Technology*, MRS Symposia Proceedings No. 467 (AIP, New York, 1997), p. 283.
[28] S. B. Concari, R. H. Butrago, M. T. Gutiener, and J. J. Gandia, J. Appl. Phys. **94**, 2417 (2003).
[29] T. Kamiya, K. Nakahata, Y. T. Ton, Z. A. K. Durrani, and I. Shimizu, J. Appl. Phys. **89**, 6265 (2001).
[30] P. G. Lecomber, G. Willeke, and W. E. Spear, J. Non-Cryst. Solids **59-60**, 795 (1983).
[31] T. Weis, S. Brehme, P. Konschat, W. Fuhs, R. Lipperheide, and U. Wille, J. Non-Cryst. Solids **299-302**, 380 (2004), and references therein.
[32] F. Liu, M. Zhu, Y. Feng, Y. Han, and J. Liu, Thin Solid Films **395**, 97 (2001).
[33] K. Shimakawa, J. Mater. Sci.: Mater. Electron. **15**, 63 (2004)
[34] F. Siebke, S. Yato, Y. Hishikawa, and M. Tanaka, J. Non-Cryst. Solids **227-230**, 977 (1998).
[35] D. Das, M. Jara, A. K. Baruo, S. Chattopodhyay, L. C. Chen, and K. H. Chen, Jpn. J. Appl. Phys., Part 2 **41**, L229 (2002).
[36] A. J. Houtepen, D. Kockmann, and D. Vanmaekelbergh, Nano Lett. **8**, 3516 (2008).
[37] I. Balberg, Y. Dover, R. Naidis, J. P. Conde, and V. Chu, Phys. Rev. B **69**, 035203 (2004).
[38] D. Azulay, I. Balberg, V. Chu, J. P. Conde, and O. Millo, Phys. Rev. B **71**, 113304 (2005).
[39] I. Balberg, L. F. Fonseca, S. Z. Weisz, J. P. Conde, P. Alpuinim, and V. Chu, Phys. Rev. B **63**, 113201 (2001).
[40] J. P. Conde, P. Brogueira, R. Castanha, and V. Chu, *Amorphous Silicon Technology*, MRS Symposia Proceedings No. 420 (AIP, New York, 1996), p. 357; J. P. Conde, P. Brogueira, and V. Chu, Philos. Mag. B **76**, 299 (1997).
[41] T. Kamei and T. Wada, Appl. Phys. Lett. **79**, 1373 (1996).
[42] Y. Posada, I. Balberg, L. F. Fonseca, O. Resto, and S. Z. Weisz, *Microcrystalline and Nanocrystalline Semiconductor Materials and Structures*, MRS Symposia Proceedings No. 638 (AIP, New York, 2001), p. F14.44.
[43] M. Mars, M. Fathallah, E. Tresso, and S. Fenero, J. Non-Cryst. Solids **299-302**, 133 (2002).
[44] G. Morell, R. S. Katiyar, S. Z. Weisz, H. Jia, J. Shinar, and I. Balberg, J. Appl. Phys. **78**, 5120 (1995).
[45] I. Balberg, J. Phys. D: Appl. Phys. **42**, 064003 (2009).
[46] H. Hadjadj, N. Pham, P. Roca i Cabarrocas, and O. Jbara, Appl. Phys. Lett. **94**, 061909 (2009).
[47] R. H. Bube, *Photoelectronic Properties of Semiconductors* (Cambridge University Press, Cambridge, 1992).
[48] D. Will, C. Lerner, W. Fuhs, and K. Lips, *Amorphous and Microcrystalline Silicon Technology*, MRS Symposia Proceedings No. 467 (AIP, New York, 1997), p. 361.
[49] D. Cavalcoli, A. Cavallini, M. Rossi, and S. Pizzini, Semiconductors **41**, 421 (2007).
[50] B. Rezek, J. Stuchlik, A. Fejfar, and J. Kocka, Appl. Phys. Lett. **74**, 1475 (1999); J. Appl. Phys. **92**, 587 (2002), and references therein.
[51] O. Millo, D. Katz, Y.-W. Cao, and U. Banin, Phys. Rev. Lett. **86**, 5751 (2001).
[52] K. Lips, P. Kanschat, and W. Fuhs, Sol. Energy Mater. Sol. Cells **78**, 513 (2003).
[53] P. U. Jensen, W. Scharier, I. H. Libon, U. Lemmer, N. E. Hecker, M. Birkholz, K. Lips, and M. Schall, J. Appl. Phys. **79**, 1291 (2001).
[54] B. G. Budagun, A. A. Aivazov, A. G. Radoselsky, and A. A. Popov, *Amorphous and Microcrystalline Silicon Technology*, MRS Symposia Proceedings No. 467 (AIP, New York, 1997), p. 239.
[55] A. Dussan, R. H. Buitrago, and R. R. Koropecki, Microelectron. J. **39**, 1292 (2008).
[56] G. H. Bauer, F. Voigt, R. Carius, M. Krause, R. Bruggemann, and T. Unold, J. Non-Cryst. Solids **299-302**, 153 (2002).
[57] J.-H. Yoon, J.-Y. Lee, and D.-H. Park, J. Non-Cryst. Solids **338-340**, 465 (2004).
[58] M. H. Brodsky, R. S. Title, K. Weiser, and G. D. Pettit, Phys. Rev. B **1**, 2632 (1970).
[59] H. Fritzsche, B.-G. Yoon, D.-Z. Chi, and M. Q. Tran, J. Non-Cryst. Solids **141**, 123 (1992).
[60] Y. Lubianiker, I. Balberg, L. Fonseca, and S. Z. Weisz, *Amorphous and Microcrystalline Silicon Technology*, MRS Symposia Proceedings No. 467 (AIP, New York, 1997), p. 209; H. L. Fonseca, S. Z. Weisz, R. Rapaport, and I. Balberg, *Amorphous and Heterogeneous Silicon Thin Films: Foundamentals*, MRS Symposia Proceedings No. 557 (AIP, New York, 1999), p. 439.
[61] J. Lu, M. Wagener, G. Rozgonyi, J. Rand, and R. Jonczyk, J. Appl. Phys. **94**, 140 (2003).
[62] M. Taguchi, Y. Tsutsumi, R. N. Bhatt, and S. Wagner, J. Non-Cryst. Solids **198-200**, 899 (1996).
[63] K. Shimakawa and A. Ganjoo, Phys. Rev. B **65**, 165213 (2002).
[64] J.-H. Zhou, S. D. Baranovski, S. Yamasaki, K. Ikuta, K. Tanaka, M. Kondo, A. Matsuda, and P. Thomas, Phys. Status Solidi B **205**, 147 (1998).
[65] A. Di Nocera, M. N. Mittiga, and A. Rubino, J. Appl. Phys. **78**, 3955 (1995).
[66] S. Shimakawa, J. Non-Cryst. Solids **352**, 1180 (2006).
[67] K. Lips, P. Kaschat, D. Will, and W. Fuhs, J. Non-Cryst. Solids **227-230**, 1021 (1998).
[68] P. Hapke, U. Backhausen, R. Carius, F. Finger, and S. Ray, *Amorphous Silicon Technology*, MRS Symposia Proceedings No. 420 (AIP, New York, 1996), p. 789.
[69] A. Dussan and R. H. Buitrago, J. Appl. Phys. **97**, 043711 (2005).
[70] J. Müller, F. Finger, R. Carius, and H. Wagner, Phys. Rev. B **60**, 11666 (1999).
[71] H. Overhof and P. Thomas, *Electron Transport in Hydrogenated Amorphous Silicon* (Springer-Verlag, Berlin, 1989).
[72] S. J. Konezny, M. N. Bussac, and L. Zuppiroli, Appl. Phys. Lett. **92**, 012107 (2008).
[73] F. Finger, J. Muller, C. Malten, R. Carius, and H. Wagner, J. Non-Cryst. Solids **266-269**, 511 (2000).
[74] C. E. Nebel, M. Rother, M. Stutzmann, C. Summonte, and M. Heintze, Philos. Mag. Lett. **74**, 455 (1996).
[75] F. Finger, C. Malten, P. Hapke, R. Carius, R. Fluckinger, and H. Wagner, Philos. Mag. Lett. **70**, 247 (1994).
[76] D. Ruff, H. Mell, L. Toth, I. Sieber, and W. Fuhs, J. Non-Cryst. Solids **227-230**, 1011 (1998).
[77] R. Brüggemann and C. Main, Phys. Rev. B **57**, R15080 (1998).
[78] J. Muller, F. Finger, R. Carius, and H. Wagner, *Amorphous and*

Microcrystalline Silicon Technology, MRS Symposia Proceedings No. 507 (AIP, New York, 1998), p. 751.
[79] S. Grebner, P. Popovic, J. Furlan, Q. Gu, and R. Schwarz, *Amorphous Silicon Technology*, MRS Symposia Proceedings No. 420 (AIP, New York, 1996), p. 795.
[80] P. Hapke, F. Finger, R. Carius, H. Wagner, K. Prasad, and R. Fluckinger, J. Non-Cryst. Solids **164-166**, 981 (1993).
[81] Z. Liu, K. Pan, Q. Zhang, M. Liu, R. Jia, Q. Lu, D. Wange, Y. Bai, and T. Li, Thin Solid Films **468**, 291 (2004).
[82] N. H. Nickel and M. Rakel, Phys. Rev. B **65**, 041301 (2001).
[83] V. Svrcek, A. Fejfar, P. Pojtik, T. Mates, A. Poruba, H. Stuchlikova, I. Palent, J. Kocka, Y. Nasuno, M. Kondo, and A. Matsuda, J. Non-Cryst. Solids **299-302**, 395 (2002).
[84] A. G. Kazanskii, H. Mell, E. I. Terukov, and P. A. Forsh, Semiconductors **34**, 367 (2000).
[85] G. W. Neudeck and A. K. Malhotra, J. Appl. Phys. **46**, 2662 (1975).
[86] G. Kawachi, C. F. O. Graeff, M. S. Brandt, and M. Stutzmann, Phys. Rev. B **54**, 7957 (1996).
[87] H. Zhou and S. R. Elliot, Phys. Rev. B **48**, 1505 (1993).
[88] S. R. Elliott, *Physics of Amorphous Materials* (Longman, New York, 1990).
[89] S. Guha and K. L. Narasimhan, Thin Solid Films **50**, 151 (1978).
[90] N. Lustig and W. E. Howard, Solid State Commun. **72**, 59 (1989).
[91] D. R. Stewart, D. A. A. Ohlberg, P. A. Beck, C. N. Lau, and R. Stanley Williams, Appl. Phys. A: Mater. Sci. Process. **80**, 1379 (2005).
[92] P. Sheng, E. K. Sichel, and J. I. Gittleman, Phys. Rev. Lett. **40**, 1197 (1978).
[93] B. Fisher, K. B. Chashka, L. Patlagan, and G. M. Reisner, Phys. Rev. B **70**, 205109 (2004).
[94] R. A. Street, Adv. Phys. **25**, 397 (1976).
[95] M. Kapoor, V. A. Singh, and G. K. Johri, Phys. Rev. B **61**, 1941 (2000).
[96] S. Lombardo, S. U. Campisano, and F. Baroetto, Phys. Rev. B **47**, 13561 (1993).
[97] J. Y. W. Seto, J. Appl. Phys. **46**, 5247 (1975).
[98] G. Baccarani, J. Appl. Phys. **49**, 5565 (1978).
[99] J. Kocka, H. Stuchlikova, J. Stuchlik, B. Rezek, T. Mates, V. Svreck, P. Fojtik, I. Palent, and A. Fejfar, J. Non-Cryst. Solids **299-302**, 355 (2002).
[100] Y. Lubianiker and I. Balberg, Phys. Status Solidi B **205**, 119 (1998).
[101] M. Hamasaki, T. Adachi, S. Wakayama, and M. Kikuchi, Solid State Commun. **21**, 591 (1977).
[102] M. H. Cohen, H. Fritzsche, and S. R. Ovshinsky, Phys. Rev. Lett. **22**, 1065 (1969).
[103] G. Juška, K. Arlauskas, M. Viliunas, and J. Kocka, Phys. Rev. Lett. **84**, 4946 (2000).
[104] W. Fuhs, P. Kanschat, and K. Lips, J. Vac. Sci. Technol. B **18**, 1792 (2000).
[105] M. L. Tarng, J. Appl. Phys. **49**, 4069 (1978).
[106] S. K. O'Leary and P. K. Lim, Solid State Commun. **101**, 513 (1997).
[107] I. J. Youngs, IEEE Trans. Dielectr. Electr. Insul. **14**, 1145 (2007).
[108] Y. Lubianiker, J. D. Cohen, H. C. Jin, and J. R. Abelson, Phys. Rev. B **60**, 4434 (1999).
[109] M. A. Paesler, D. A. Anderson, E. C. Freeman, G. Moddel, and W. Paul, Phys. Rev. Lett. **41**, 1492 (1978).
[110] K. Winer, J. Vac. Sci. Technol. B **7**, 1226 (1989).
[111] S. Veprek, Z. Iqbal, R. O. Kuhne, P. Canezzto, F. A. Sarott, and J. K. Gimzewski, J. Phys. C **16**, 6241 (1983).
[112] X. L. Xu, J. Electron. Mater. **22**, 2008 (1993).
[113] W. A. Turner and G. Lucovsky, *Amorphous Silicon Technology*, MRS Symposia Proceedings No. 297 (AIP, New York, 1993), p. 521.
[114] T. Kamei and T. Wada, J. Appl. Phys. **96**, 2087 (2004).
[115] R. Brüggeman, A. Hierzenberger, P. Reinig, M. Rojahn, M. B. Schubert, S. Schweizer, H. N. Wanka, and I. Zrinscak, J. Non-Cryst. Solids **227-230**, 982 (1998).
[116] T. J. McMahan and R. S. Crandall, Phys. Rev. B **39**, 1766 (1989).
[117] M. Aoucher, J. Mohammad-Brahim, and B. Fortin, J. Appl. Phys. **79**, 7041 (1996).
[118] J. Hautala and J. D. Cohen, J. Non-Cryst. Solids **164-166**, 371 (1993).
[119] E. H. Nicolian and J. R. Brown, *MOS (Metal Oxide Semiconductors) Physics and Technology* (Wiley, New York, 1982).
[120] I. Balberg, D. Azulay, D. Toker, and O. Millo, Int. J. Mod. Phys. B **18**, 2091 (2004).
[121] A. Heya, A.-Q. He, N. Otsuka, and H. Matsumura, J. Non-Cryst. Solids **227-230**, 1016 (1998).
[122] Y. Lubianiker and I. Balberg, Phys. Rev. Lett. **78**, 2433 (1997).
[123] S. J. Bending and M. R. Beasley, Phys. Rev. Lett. **55**, 324 (1985).
[124] T. Weis, R. Lipperheide, U. Wille, and S. Brehme, J. Appl. Phys. **92**, 1411 (2002).
[125] P. Kanschat, K. Lips, R. Bruggemann, A. Hierzenberger, I. Seiber, and W. Fuhs, *Amorphous and Microcrystalline Silicon Technology*, MRS Symposia Proceedings No. 507 (AIP, New York, 1998), p. 793.
[126] I. P. Zvyagin, I. A. Kurova, M. A. Nal'gieva, and N. N. Ormont, Semiconductors **40**, 108 (2006).
[127] Y. Furuta, H. Mizuta, K. Nakazato, T. T. Yong, T. Kamiya, Z. Durrani, H. Ahmed, and K. Taniguchi, Jpn. J. Appl. Phys., Part 2 **40**, L615 (2001).
[128] F. Diehl, M. Scheib, B. Schroder, and H. Oechsner, J. Non-Cryst. Solids **227-230**, 973 (1998).
[129] T. Dylla, F. Finger, and E. A. Schiff, Appl. Phys. Lett. **87**, 032103 (2005).
[130] C. A. Dimitriadis, J. Appl. Phys. **73**, 4086 (1993).
[131] G. A. Armstrong, Solid-State Electron. **41**, 835 (1997).
[132] I. Balberg, E. Savir, and J. Jedrzejewski (unpublished).
[133] See, for example, T. J. King, M. G. Hack, and I. W. Wu, J. Appl. Phys. **75**, 908 (1994).
[134] H. Fujiwara, M. Kondo, and A. Matsuda, Phys. Rev. B **63**, 115306 (2001).
[135] S. Ishida, S. Takaoka, K. Oto, K. Murase, S. Shirai, and T. Serikawa, J. Non-Cryst. Solids **198-200**, 1125 (1996).
[136] B. Ruttensperger, G. Muller, and G. Krotz, Philos. Mag. B **68**, 203 (1993).
[137] R. Vanderhaghen, S. Kasouit, R. Brenot, V. Chu, J. P. Conde, F. Liu, A. de Martino, P. Roca, and I. Cabarrocas, J. Non-Cryst. Solids **299-302**, 365 (2002).
[138] A. L. Fripp, J. Appl. Phys. **46**, 1240 (1975).
[139] T. Kamiya, Y. Furuta, Y. T. Tan, Z. A. K. Durrani, H. Mizuta, and H. Ahemed, Solid State Phenom. **93**, 345 (2003).
[140] F. Mares, A. Fejfar, I. Drbohlav, B. Rezrk, P. Fojtik, K.

Luterova, J. Kocka, C. Koch, M. B. Schubert, M. Ito, K. To, and H. Uyama, J. Non-Cryst. Solids **299-302**, 767 (2002).
[141] I. Balberg and N. Binenbaum, Phys. Rev. B **35**, 8749 (1987).
[142] A. Smith and S. Torquato, J. Appl. Phys. **65**, 893 (1989).
[143] T. Unold, R. Bruggemann, J. P. Kleider, and C. Longeaud, J. Non-Cryst. Solids **266-269**, 325 (2000).
[144] J. J. Schellenberg and R. D. McLeod, Solid State Commun. **66**, 159 (1988).